PHOTOCHEMICALLY PRODUCED REACTIVE SPECIES GENERATION BY EXTRACELLULAR ORGANIC MATTER SENSITIZERS FROM *CHLAMYDOMONAS REINHARDTII*

BY

RAUL TENORIO

THESIS

Submitted in partial fulfillment of the requirements
for the degree of Master of Science in Environmental Engineering in Civil Engineering
in the Graduate College of the
University of Illinois at Urbana-Champaign, 2015

Urbana, Illinois

Advisers:

Professor Timothy J. Strathmann
Assistant Professor Jeremy S. Guest

ABSTRACT

Microalgae biotechnologies have shown promise as tertiary wastewater treatment processes capable of reducing nitrogen and phosphorous to meet increasingly stringent regulatory limits and as producers of biofuel feedstock. During growth and respiration, microalgae excrete extracellular organic matter (EOM) as metabolic byproducts which have the potential to act as photosensitizers for the generation of reactive species, including singlet oxygen ($^1O_2$), hydroxyl radicals (•OH), and triplet excited dissolved organic matter (^{3}DOM). These reactive species can play an essential role in the mineralization of dissolved organic matter, nutrient cycling and bioavailability, attenuation of toxic pollutants, and inactivation of pathogens. Recent studies observed enhanced transformation of organic micropollutants in UV and visible light irradiated algae suspensions where photogenerated $^1O_2$ and •OH were detected. The photochemistry in EOM matrices is still largely unknown as well as the impacts of reactive species on cultivation including EOM mineralization, protective extracellular reactive species generation, and nutrient availability. This study reports on reactive species production in EOM solutions separated from pure batch cultures of *Chlamydomonas reinhardtii* under solar irradiation. Results show increasing steady-state levels of ^{3}DOM, $^1O_2$, and formation rates of •OH under sunlight irradiation as EOM levels increase with batch culture growth. Changes in reactive species levels were compared with changes in culture characteristics such as volatile suspended solids (VSS) and nutrient availability as well as EOM properties including dissolved organic carbon (DOC) and specific UV absorbance (SUVA). EOM-sensitized reactive species photogeneration in comparison to other DOM sources was also discussed along with implications for the fate of contaminants, EOM, and culture stability in photobioreactors.

TABLE OF CONTENTS

CHAPTER 1: INTRODUCTION

1.1 Extracellular photochemistry in phototrophic cultivation systems

Photochemistry of the extracellular environment in algal cultivation systems is largely unknown. Algal technologies have shown promise as producers of algae feedstock for biofuel production (U.S. Department of Energy, 2010) as well as tertiary wastewater treatment processes capable of reducing nitrogen and phosphorous (McGriff Jr. and McKinney, 1972; Muñoz and Guieysse, 2006; Oswald, 1991, 1995). Photoautotrophic algae cultivation designs vary from open ponds to closed photobioreactors (PBRs), all of which require light to drive photosynthesis (U.S. Department of Energy, 2010). While much is known about photosynthesis and the photochemical processes that occur inside of an algal cell (Minagawa, 2009), the photochemistry occurring outside of the cell in the extracellular water matrix is still mostly unknown, despite potential relevance to the stability of cultures, nutrient cycling, contaminant fate, and pathogen inactivation among other things.

Of particular interest is the generation of photochemically produced reactive species which include the well-studied subset reactive oxygen species (ROS). In terrestrial dissolved organic matter (DOM), reactive species play important roles in DOM mineralization, persistent pollutant attenuation, pathogen inactivation, and nutrient bioavailabity (Buxton et al., 1988; Cory et al., 2010; Davies-Colley et al., 1999; Foote, 1995; Gerecke et al., 2001; Loiselle et al., 2012; Scully Jr. and Hoigné, 1987; Zuo and Jones, 1997). Yet few studies have examined the photogeneration of reactive species in algal photobioreactor cultures which can contain dense biomass and high concentrations of algal organic matter (AOM) (de Godos et al., 2012); some studies have reported EOM levels as high as 70 mg/L as dissolved organic carbon during stationary phase (Pivokonsky et al., 2014). Reactive species play an important role driving many chemical

processes in sunlit natural waters (Foote, 1995) and may play analogous roles in cultivation systems, however this knowledge is unknown. The disconnect between reactive species quantification techniques which have been established and refined since the 1980s (Foote, 1995) and algal PBR design which has been discussed since the 1990s (Oswald, 1991, 1995) must converge to uncover a deeper understanding of photobioreactor photochemistry.

1.2 The importance of photogenerated reactive species in algal systems

Photochemically produced reactive species are transient intermediates with short lifetimes (e.g., microseconds or less) that are essential for a multitude of chemical processes in natural waters that promote ecosystem stability (Burns et al., 2012; Foote, 1995). The reactive species involved in these processes include singlet oxygen ($^1O_2$), hydroxyl radicals (•OH), superoxide ($O_2^{\bullet-}$), hydrogen peroxide (H_2O_2), and carbonate radicals ($CO_3^{\bullet-}$), and triplet excited dissolved organic matter (^{3}DOM) (Burns et al., 2012; Foote, 1995; Grandbois et al., 2008; Leifer, 1988).

Photogenerated reactive species play a role in carbon mineralization and can also convert biologically-inert higher molecular weight organic compounds into more easily metabolized fractions via oxidative cleavage reactions (Foote, 1995), leading to production of lower weight carboxylic acids, CO, and CO_2 (Goldstone et al., 2002; Page et al., 2014; Zuo and Jones, 1997) (Cory et al., 2010; Loiselle et al., 2012; Peterson et al., 2012).

Reactive species can also promote indirect photolysis and natural attenuation of toxic organic pollutants (Burns et al., 2012; Chen et al., 2009; Dalrymple et al., 2010; Halladja et al., 2007). Of the reactive species listed, •OH, $^1O_2$, and ^{3}DOM have been studied more closely for their ability to oxidize pollutants and inactivate pathogenic microorganisms (Buxton et al., 1988; Davies-Colley et al., 1999; Halladja et al., 2007; Housari et al., 2010; Rosado-Lausell et al., 2013, 2013;

Scully Jr. and Hoigné, 1987; Timko et al., 2014). Hydroxyl radicals are the strongest oxidant in the above mentioned list and react unselectively with natural organic matter and many synthetic organic chemicals at rates approaching diffusion limitations (Buxton et al., 1988). Singlet oxygen is more selective and reacts with furan, phenoxide anion, phenol, sulfur, and alkene functional groups present in many micropollutants (Mostafa and Rosario-Ortiz, 2013; Peterson et al., 2012; Scully Jr. and Hoigné, 1987). Reactions with some of the same functional groups leads to inactivation of many pathogens, including MS2 coliphage, enterococci, and fecal coliforms (Davies-Colley et al., 1999; Kohn and Nelson, 2007; Kohn et al., 2007; Mostafa and Rosario-Ortiz, 2013; Romero et al., 2011). Like $^1O_2$, ^{3}DOM is a selective oxidant; recent studies have shown the ^{3}DOM photoproduction leads to oxidation of contaminants of emerging concern, including sulfa drugs and phenyl urea herbicides (Boreen et al., 2005; Dalrymple et al., 2010; Gerecke et al., 2001; Guerard et al., 2009).

Reactive species are also crucial for making nutrients bioavailable in natural waters (Foote, 1995). Reaction of DOM with •OH can release organic nitrogen and ammonia, making nitrogen available for microorganisms (Bushaw et al., 1996; Janssen et al., 2014). $O_2^{\bullet-}$ exhibits both reducing and oxidizing potential and has been shown to play a prominent role in trace metal biogeochemical cycling in sunlit aquatic systems (Goldstone and Voelker, 2000; Petasne and Zika, 1987; Voelker et al., 2000).

Not only is DOM a sensitizer for the reactive species discussed above, this same DOM source is a sink for several reactive species. For example, aromatic ketones and quinones, which are known precursors for ^{3}DOM photogeneration, can also serve as quenchers for ^{3}DOM (Wenk and Canonica, 2012). Similarly, one recent study found that DOM in arctic aquatic ecosystems was the dominant source and sink for •OH. Quantum yields for •OH quenching were 10 – 100-fold

greater than quantum yields for •OH production, suggesting a dominant quenching role in the arctic DOM systems investigated (Page et al., 2014). In contrast, aquatic DOM at environmentally relevant conditions is known to be primarily a source for $^1O_2$ contributing negligible quenching (Cory et al., 2009; Mostafa and Rosario-Ortiz, 2013).

Whereas the importance of photochemical reactions in natural extracellular aquatic systems has long been recognized, potentially equally important processes in EOM-rich algae cultivation systems remain largely unknown. Terrestrial DOM and algal organic matter are similar in water matrix composition. Photobioreactors contain inorganic constituents in media which are used by algal cells to sustain biomass growth including inorganic carbon, nitrogen, phosphorous, and trace metals (Andersen, 2005). Algae also produce metabolic excretions throughout growth (Henderson et al., 2008; Nguyen et al., 2005; Pivokonsky et al., 2014). Therefore, the extracellular organic matter (EOM) becomes the DOM source available for photochemical reactions in photobioreactors analogous to the terrestrial DOM sensitizers in natural waters.

The photoreactivity of AOM has not been studied closely regardless of the clear parallel drawn between both natural waters and photobioreactors. And as a result, the impacts of reactive species on biomass yield or culture stability are not understood. Do reactive species play a significant role in mineralization, oxidizing organic compounds, and pathogen inactivation similar to natural waters? Is there an inhibiting or beneficial effect to culture growth? These are the important questions that must be addressed. Fortunately, much work has been done in DOM photochemistry and AOM characterization, so this knowledge can be leveraged together with targeted experimentation to gain a greater understanding of this unknown water matrix.

1.3 State of knowledge

The steady-state concentrations of $^1O_2$, •OH, and ^{3}DOM in sunlit natural waters have been quantified using molecular probes (Canonica and Freiburghaus, 2001; Canonica et al., 1995; Foote, 1995; Grebel et al., 2011). Steady-state concentrations in natural waters were measured and typical values are as follows: $[^1O_2] = 10^{-13} – 10^{-12}$ M; [•OH] = $10^{-18} – 10^{-15}$ M; $[^3DOM] = 10^{-15} – 10^{-13}$ M (Burns et al., 2012; Zepp et al., 1985a).

Researchers have worked to elucidate the structural elements in terrestrial DOM sensitizers that are responsible for reactive species formation and quenching. Singlet oxygen has been shown to form after sensitization of aromatic ketone groups in natural organic matter (Golanoski et al., 2012; Sharpless, 2012). Hydroxyl radicals are generated from electron and energy transfer reactions with ^{3}DOM, although this pathway is not well understood (Page et al., 2014). And triplet excited state dissolved organic matter originates from sensitization of aromatic ketones, aldehydes and quinone functional groups (Canonica and Freiburghaus, 2001; Golanoski et al., 2012; Janssen et al., 2014). In addition to identifying reactive species precursors, researchers have made efforts to use bulk terrestrial DOM characteristics such as absorbance, fluorescence, and DOC to identify key DOM characteristics and photosensitizing capabilities (Sharpless, 2012).

The effects of suspended organic matter particles on photochemical transformation of organic contaminants in natural waters inspired Zepp and coworkers to begin one of the first investigations linking microalgae to photochemical organic contaminant removal (Zepp and Schlotzhauer, 1983). The presence of green microalgae species including *Chlamydomonas sp.* and *Chlorogonium sp.* were found to enhance the removal of pesticides, herbicides, and other

organic pollutants compared to direct UV and visible light photolysis alone (Zepp and Schlotzhauer, 1983). More recent studies have built on the findings by Zepp and Schlotzhauer and showed that microalgae cell suspensions under UV and visible light also exhibit enhanced transformation of pharmaceuticals and personal care products (PPCPs) and other micropollutants (Ge et al., 2009; Wang et al., 2007). After detecting $^1O_2$ and •OH in irradiated microalgae suspensions, researchers believe photochemically produced reactive species are a major contributor to enhanced contaminant transformation observed in these systems (Liu et al., 2004; Wang et al., 2007; Zhang et al., 2012).

In recent years, there has also been an increased interest in characterizing AOM (Henderson et al., 2008; Li et al., 2012; Nguyen et al., 2005; Pivokonsky et al., 2014). To organize the different fractions of AOM, the material has been divided into three operationally defined categories: intracellular organic matter, extracellular organic matter, and cellular organic matter (Henderson et al., 2008; Pivokonsky et al., 2014). Intracellular organic matter (IOM) consists of the soluble organic matter inside of but not including the cell wall (Henderson et al., 2008). Extracellular organic matter (EOM) refers to the dissolved metabolic excretions of microalgae (Henderson et al., 2008; Li et al., 2012; Pivokonsky et al., 2014). Cellular organic matter (COM) has been defined as the cell wall and organelles, or the solid portion of algal cells (Pivokonsky et al., 2014). Compositional changes in AOM from algal cultures when comparing exponential and stationary growth has been a common observation in these studies (Henderson et al., 2008; Nguyen et al., 2005; Pivokonsky et al., 2014). The motivation behind AOM characterization to date has been to understand the physical and chemical properties. The presence of AOM in drinking water sources is often seen as a nuisance material that creates taste and odor issues, increases coagulant demand, leads to greater membrane fouling, and produces disinfection

byproducts (Henderson et al., 2008; Li et al., 2012; Nguyen et al., 2005; Pivokonsky et al., 2014). The connection to photoreactivity in algal cultivation systems has not been made.

The development of DOM characterization and reactive species quantification techniques in terrestrial NOM has given researchers a set of tools that can be applied in a diverse array of organic matter present in engineered and natural systems such as wastewater organic matter, microbial derived organic matter from Antarctic lakes, and algal cell suspensions (Brown et al., 2004; Dong and Rosario-Ortiz, 2012; Jasper and Sedlak, 2013; Liu et al., 2004; Niu et al., 2014; Quaranta et al., 2012; Ryan et al., 2011; Wang et al., 2007; Zhang et al., 2012). By using these tools, researchers were able to understand the photoreactivity of exotic organic matter sources and evaluate the reactive species generating performance in these systems.

1.4 A gap in understanding

Currently, only a few studies have proposed AOM sensitization as a reactive species generating pathway (Ge et al., 2009; de Godos et al., 2012; Liu et al., 2004; Peng et al., 2006; Zhang et al., 2012). And even fewer studies have quantified reactive species in AOM solutions and only •OH and $^1O_2$ were quantified (Liu et al., 2004; Wang et al., 2007; Zhang et al., 2012). So, the existing knowledge on AOM photoreactivity which we can directly apply to sunlit algae cultivation systems is lacking and needs to be addressed.

Algal biotechnology has created an intersection between both the knowledge of AOM characterization and reactive species quantification, so both ideas must be applied to advance the quantitative understanding of the photochemistry inside photobioreactors. The advantage of utilizing methods from an established body of literature in DOM photochemistry is that it is possible to assess the reactive species generating performance of AOM by comparing findings to

those of terrestrial DOM. Therefore, DOM information should be used as a baseline for performance. Photoreactivity comparisons must then be traced back to the characteristics of each organic matter to distinguish differences in organic matter properties and attribute those differences to changes in reactive species production.

AOM characteristics in photobioreactors are not static, and photoreactivity is expected to change throughout culture age. A deeper understanding of AOM photoreactivity requires analysis of AOM as it evolves throughout growth. Identifying factors such as water quality characteristics, culture growth, and growth stage which affect photoreactivty can further advance our understanding of reactive species generation in photobioreactors. For example, does the photosensitizing property of EOM produced at different growth stages differ?

Only after quantifying production of reactive species in photobioreactors can we begin understand their potential influence on the fate of micropollutants, pathogens, and AOM itself in algal cultivations systems. Is AOM primarily a light absorber and defense mechanism that stabilizes growth, a quencher that prevents excessive oxidation of algal cells, a sensitizer that attacks harmful pollutants and pathogens via indirect photolysis? Improved quantitative understanding of extracellular photochemistry in PBRs can help to address these important questions.

1.5 Integrating algal cultivation with photochemistry

Since the questions posed above are broad and have uncertain outcome, the most pertinent information that must be obtained are the AOM derived reactive species levels produced by EOM photosensitization in photobioreactors. Therefore, reactive species concentrations and formation rates served as the quantitative measures of AOM photoreactivity in this study.

Efforts were focused around investigating the photogeneration of •OH, ^{3}DOM, and $^1O_2$ in sunlight-irradiated EOM. Chromophoric dissolved organic matter (CDOM), or DOM that has a brown/yellow color and absorbs light, is the basis for reactive species generation in terrestrial DOM (Blough and Zepp, 1996; Richard and Canonica, 2005; Zafiriou et al., 1984). EOM is the AOM most comparable with terrestrial DOM when considering all three fractions (IOM, EOM, and COM) since it is completely dissolved and also light-absorbing. Additionally, EOM is the most practical AOM to investigate since widely available organic matter characterization, reactive species quantification, and experimental techniques developed for DOM can be directly applied in EOM investigation.

Specifically, experiments were conducted to measure photoproduction of •OH, ^{3}DOM, and $^1O_2$ in simulated sunlight irradiated batches of EOM isolated from pure batch cultures of *C. reinhardtii* at different stages of growth. To the best of our knowledge, this is the first study investigating reactive species generation by EOM produced throughout exponential and stationary phase in engineered photobioreactor systems. •OH, ^{3}DOM, and $^1O_2$ were quantified using molecular probes benzene, 2,4,6-trimethyl phenol (TMP), and furfuryl alcohol (FFA) respectively. Changes in reactive species levels were compared with changes in culture characteristics such as volatile suspended solids (VSS) and nutrient availability as well as EOM properties, including dissolved organic carbon (DOC) and specific UV absorbance (SUVA). EOM-sensitized reactive species production was compared to Suwannee River Natural Organic Matter (SRNOM), a commonly studied terrestrial DOM isolate. This comparison enables translation of the developed body of knowledge from terrestrial DOM systems to dense cell microalgae processes.

CHAPTER 2: MATERIALS AND METHODS

2.1 Chemical reagents

All chemicals were used as received. Benzene (BZ; 99.8%, Sigma-Aldrich), 2,4,6-trimethylphenol (TMP; 97%, Sigma-Aldrich), and furfuryl alcohol (FFA; 99%, Sigma-Aldrich) were used as molecular probes for quantifying reactive species. Media was prepared from NH_4Cl (ACS Grade, Amresco), $MgSO_4•7H_2O$ (≥ 99.5%, Fluka), $CaCl_2•H_2O$ (≥ 99.5%, Fluka), K_2HPO_4 (≥ 98%, Sigma-Aldrich), KH_2PO_4 (≥ 98%, Sigma-Aldrich), EDTA (≥ 99%, Sigma-Aldrich); $(NH_4)6Mo_7O_{24}•4H_2O$ (ACS Grade, Acros Organics), Na_2SeO_3 (98%, Sigma-Aldrich), $ZnSO_4•7H_2O$ (≥ 99%, Sigma-Aldrich), $MnCl_2•4H_2O$ (99%, Sigma-Aldrich), Na_2CO_3 (≥ 99.95%, Sigma-Aldrich), $FeCl_3•6H_2O$ (97%, Sigma-Aldrich), $CuCl_2•2H_2O$ (≥ 99.5%, Sigma-Aldrich), and $NaHCO_3$ (100%, Fisher Scientific). All pH and ionic strength adjustments were made using HCl (ACS Grade, Macron Fine Chemicals), NaOH (1 N Solution, Sigma-Aldrich), and NaCl (ACS Grade, Fisher Scientific). Suwannee River Natural Organic Matter (SRNOM) (reverse osmosis isolate) was obtained from the International Humic Substances Society and used as a representative example of terrestrial organic matter. Methanol (Fisher Scientific), acetonitrile (Macron Fine Chemicals), orthophosphoric acid (85%, Sigma-Aldrich), and acetic acid (≥ 99.7%, Sigma-Aldrich) were used to prepare eluents for liquid chromatography analysis.

2.2 *Chlamydomonas reinhardtii* cultivation and characterization

Solutions containing Extracellular Organic Matter (EOM) were obtained from a pure culture of *Chlamydomonas reinhardtii* (#2243, UTEX). *C. reinhardttii* was grown in a 5 L photobioreactor constructed from PVC and acrylic sheets (37” × 12” × 1-3/8”; see Appendix A) and was placed in front of lit blue and red LEDs at a 24-hour incident light intensity of 237 $\mu E/m^2$-s. Modified TAP media was used, omitting TRIS buffer and acetic acid to reduce DOC levels, with the

following composition (mM): NH_4Cl (7.0), K_2HPO_4 (0.620), KH_2PO_4 (0.397), $NaHCO_3$ (10), $MgSO_4 \cdot 7H_2O$ (0.406), $CaCl_2 \cdot 2H_2O$ (0.340), Na_2CO_3 (0.022), $FeCl_3 \cdot 6H_2O$ (0.020), EDTA-$Na_2 \cdot 2H_2O$ (0.058), Na_2SeO_3 (0.1 μM), $ZnSO_4 \cdot 7H_2O$ (2.5 μM), $MnCl_2 \cdot 4H_2O$ (6 μM), $CuCl_2 \cdot 2H_2O$ (2 μM). Mixing was achieved with an air pump and diffuser dispensing an air/CO_2 mixture into the reactor varying from 0.02 L/L-min at 5 L culture volume to 0.5 L/L-min at 0.1 L culture volume. The pH was maintained between 6.8 – 7.2 by injecting $CO_{2(g)}$ (99%) into the air stream through a solenoid valve (McMaster Carr) controlled by a pH controller (Eutech Instruments). All air-inlets and outlets were filtered using HEPA vent filters (Whatman) to maintain sterility. All reactor parts were sterilized before inoculation by either autoclaving or UV irradiation.

2.3 Growth monitoring

C. reinhardtii was grown in batch for 10 days, and growth was monitored throughout lag, exponential, and stationary phases. Mass concentrations of the culture were obtained using total suspended solids (TSS) and volatile suspended solids (VSS) analysis (Guest et al., 2013). Optical density was measured at 735 nm using a UV-vis spectrophotometer (DR/4000 U, HACH). Growth was initiated by inoculating 1% (v/v) inoculum into the 5 L reactor. The inoculum was obtained from a 500 mL *C. reinhardtii* batch reactor grown under the same cultivation conditions. The 5 L reactor was seeded when inoculum optical density at $\lambda = 735$ nm (A_{735}) reached ~0.8.

2.4 EOM isolation and characterization

EOM isolation has been adapted by combining two methods previously described (Henderson et al., 2008; Li et al., 2012). Approximately 600 mL of cell suspension was collected and

centrifuged (SORVALL RC 6+, Thermo Scientific) at 10,000 × g for 15 min at 20°C. Supernatant was then sequentially filtered through a 0.7 μm glass fiber membrane (Fisherbrand) and a 0.22 μm PES membrane (Steritop, Millipore). The PES filtrate is operationally defined as dissolved EOM and included media components (Henderson et al., 2008; Li et al., 2012; Nguyen et al., 2005; Pivokonsky et al., 2014). EOM solution was stored at 4 °C until used.

DOC of the EOM solution was measured using a total organic carbon (TOC) analyzer (TOC-VCPH, Shimadzu) using potassium hydrogen phthalate reference standard solution (Aqua Solutions). Alkalinity was measured by pH titration according to Standard Methods (Eaton et al., 1995). Ammonia was measured using the phenate method (Eaton et al., 1995; Guest et al., 2013). Phosphate was measured using the ascorbic acid method (Eaton et al., 1995; Guest et al., 2013). UV-vis absorbance spectra of the EOM solution was collected from λ = 250 nm - 750 nm against a deionized water blank (Shimadzu UV-2550 Spectrophotometer). All EOM solution analyses were performed within 10 days of collection.

2.5 Experimental setup and procedure for reactive species quantification

Reactive species quantification experiments were performed using an Atlas Suntest XLS+ solar simulator equipped with a xenon lamp emitting irradiation filtered through a 310 nm glass cutoff filter (Atlas, Cat. 56052372). Reactors consisted of 50 mL glass beakers with black tape wrapped around the outer surface to limit unintended light reflection (Romero et al., 2011). A 280 nm longpass cutoff filter (FSQ-WG280) was placed on top of each beaker during experiments to limit evaporation and also allow penetration of the full radiation spectrum. 300 rpm mixing was achieved using a 12-point stir plate (Variomag). Capped borosilicate glass tubes (16 × 150 mm) (Kimax) served as the reactors for •OH production rate quantification experiments to limit

benzene volatilization (Dong and Rosario-Ortiz, 2012). All reactors were placed in a water bath inside of the solar simulator chamber and temperature was maintained at 25 °C during irradiation via a copper coil also placed inside the bath which was connected to an external temperature controller (Neslab RTE 7, Thermo Electron Corporation). Solar simulator light intensity was measured by spectroradiometer to be 361 ± 47 W/m^2 (Spectrilight ILT950, International Light Technologies). The spectroradiometer sensor was placed at 12 positions corresponding to the 12-points on the stirplate where reactors were placed. Light intensity was measured and the average of triplicate measurements was recorded (see appendix for details).

•OH, ^{3}DOM, and $^1O_2$, were quantified using benzene (BZ), TMP, and FFA respectively. Two kinetic concepts were used to quantify the reactive species. The first order method was used to quantify ^{3}DOM steady-state ($[^3DOM]_{ss}$) and $^1O_2$ steady-state ($[^1O_2]_{ss}$) concentrations. The initial formation rate method was used to quantify •OH formation rates ($R^{\bullet OH}$) (see appendix). $[^3DOM]_{ss}$ was obtained by measuring TMP decay, which reacts mainly with ^{3}DOM (Canonica and Freiburghaus, 2001; Canonica et al., 1995). $[^1O_2]_{ss}$ was obtained by measuring FFA, which decays selectively with $^1O_2$ reaction (Haag and Hoigne, 1986; Haag et al., 1984). $R^{\bullet OH}$ was obtained by measuring production of phenol, a hydroxylation product of BZ (Dong and Rosario-Ortiz, 2012; Dorfman et al., 2004). To maintain consistent probe concentrations in all experiments and to accommodate probe stock solution volumes, 90% (v/v) of EOM isolate solutions were added in all reactors. EOM water quality, including DOC and alkalinity, varied throughout *C. reinhardtii* growth which changed the reactor conditions in irradiation experiments; this dynamic water quality is described later. Initial probe concentrations were $[TMP]_o$ = 10 μM, $[FFA]_o$ = 10 μM, and $[BZ]_o$ = 1 mM. ^{3}DOM experiments underwent a 4-hour irradiation period while •OH and $^1O_2$ experiments were extended to 8 hours to provide more time

for additional probe degradation and product formation after reactive species interaction. Aliquots (1 mL) were collected throughout the irradiation experiments at regular intervals, and stored in 2 mL glass vials under darkness at 4 °C until analyzed.

Terrestrial organic matter comparison experiments followed an identical reactor setup and experimental procedure as described above. Water quality parameters measured from EOM characterization in exponential phase dictated the water quality characteristics in the terrestrial organic matter surrogate matrix. Alkalinity, ionic strength, and pH were adjusted using $NaHCO_3$, NaCl, and HCl/NaOH respectively. DOC in terrestrial organic matter matrices was provided by the addition of organic carbon from a SRNOM isolate.

2.6 Analytical methods

Phenol, 2,4,6-trimethylphenol, and furfuryl alcohol were measured using high performance liquid chromatography (HPLC) equipped with a photodiode array detector (SPD-M10Avp, Shimadzu). Separation was achieved using a Spherisorb 5 μm ODS2 4.6 × 150 mm column with 4.6 × 10 mm guard cartridge of the same material. Phenol production due to benzene reaction with •OH was analyzed at λ = 270 nm using a 35/65 mixture of acetonitrile and acetic acid aqueous solution (pH = 5). TMP was analyzed at λ = 277 nm using isocratic flow with a 60/40 mixture of methanol and 10 mM orthophosphoric acid aqueous solution (pH = 2). Furfuryl alcohol was analyzed at λ = 214 nm using isocratic flow with a 20/80 mixture of acetonitrile and acetic acid aqueous solution (pH = 5).

CHAPTER 3: RESULTS AND DISCUSSION

3.1 *C. reinhardtii* growth monitoring and EOM characterization

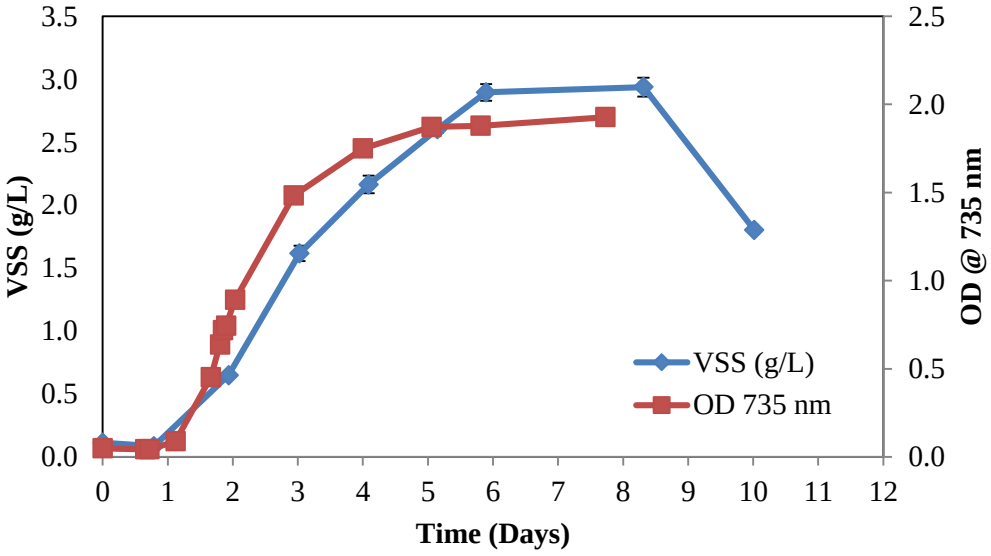

Figure 1: *C. reinhardtii* growth monitored using volatile suspended solids (VSS) analysis and optical density at λ = 735 nm.

Figure 1 shows *C. reinhardtii* growth proceeding through a lag, exponential, and stationary phase. The lag phase transitions into exponential phase at day 1. Exponential phase growth occurs from day 1 to 4 before approaching early stationary phase. Stationary growth begins on day 6 then plateaus through day 10. The decrease in VSS at day 10 likely results from poor mixing as the culture becomes denser in the photobioreactor.

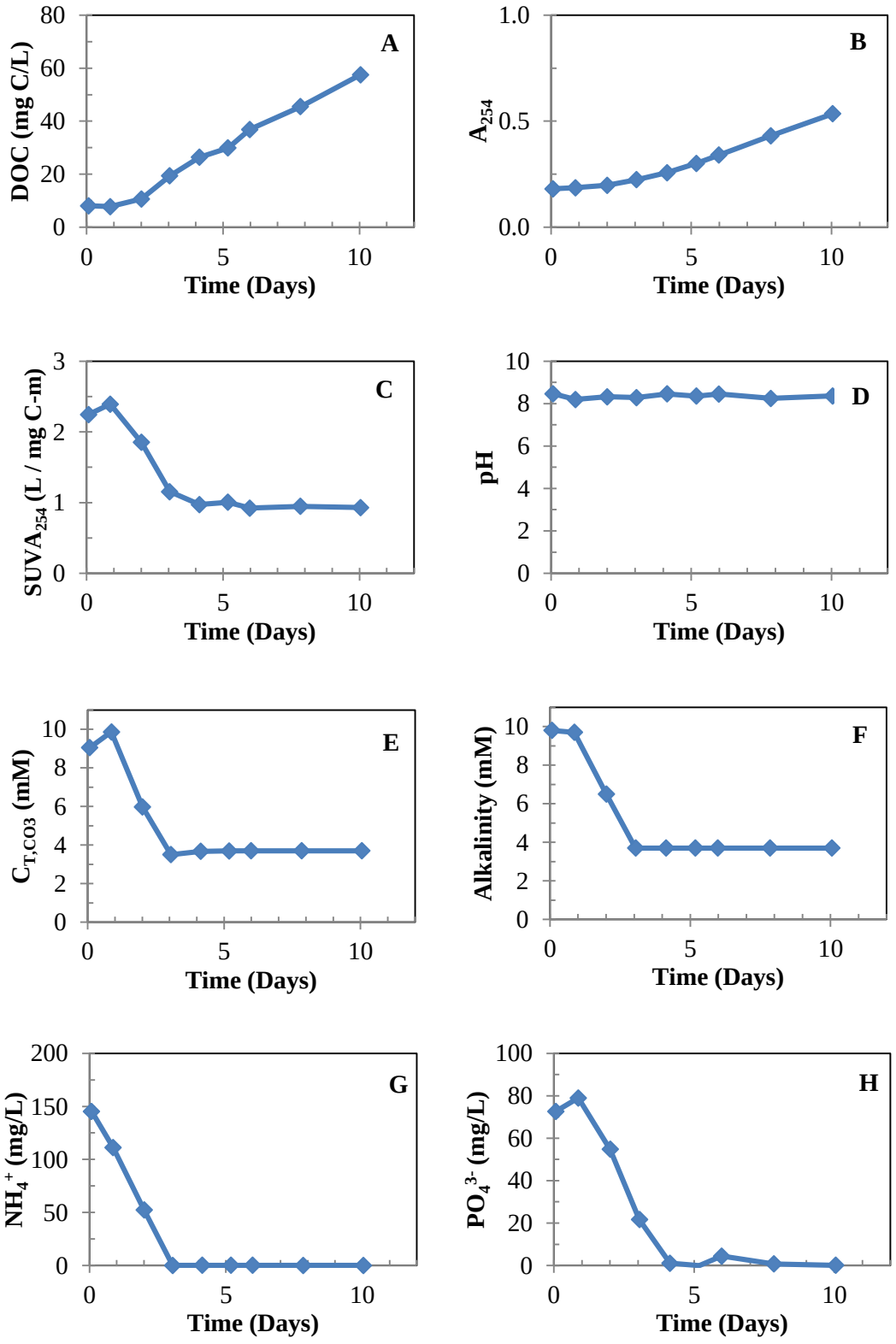

Figure 2: EOM water quality characteristics throughout 10 day cultivation period.

Figure 2 shows that DOC increases linearly over time similarly to microalgae DOC production measured in other studies (Nguyen et al., 2005; Pivokonsky et al., 2014). The culture initially starts with ~ 8 mg C/L due to the organic carbon contribution from the 6.9 mg C/L of EDTA added to the TAP media (assumed to be negligibly bioavailable) and ~1.1 mg C/L contributed from EOM in the inoculum used to seed the reactor. PO_4^{3-} and NH_4^+ decrease as growth increases in the culture due to nutrient uptake. Initially, the main carbon source is EDTA, which inflates $SUVA_{254}$ values to ~ 2.3 L / mg C-m due to formation of light absorbing chelation complexes with Fe^{3+} in the media. As extracellular materials becomes the dominant source of DOC, $SUVA_{254}$ stabilizes at around 1 L / mg C-m, closer to the actual value for SUVA for EOM. $SUVA_{254}$ below 2 L / mg C-m is considered a low value and typical of biologically derived organic matter with low aromatic content (Henderson et al., 2008). $SUVA_{254}$ has also been known to decrease from exponential to stationary phase (Henderson et al., 2008; Pivokonsky et al., 2014). The EOM solution has a pH ~ 8 throughout culture growth. However, it should be mentioned that pH in EOM solutions is different from the pH maintained in the photobioreactor (pH = 6.81 – 7.16) since culture pH is regulated using a CO_2 injection system, but not after supernatant separation. Alkalinity is dominated by the initial 10 mM $NaHCO_3^-$ added to the growth media, as displayed in Figure 2. After 3 days, the alkalinity and $C_{T,CO3}$ stabilized at 3.7 mM. The significant drop in alkalinity can be explained by HCO_3^- uptake by *C. reinhardtii* throughout growth and stabilization upon reaching stationary phase where growth plateaus.

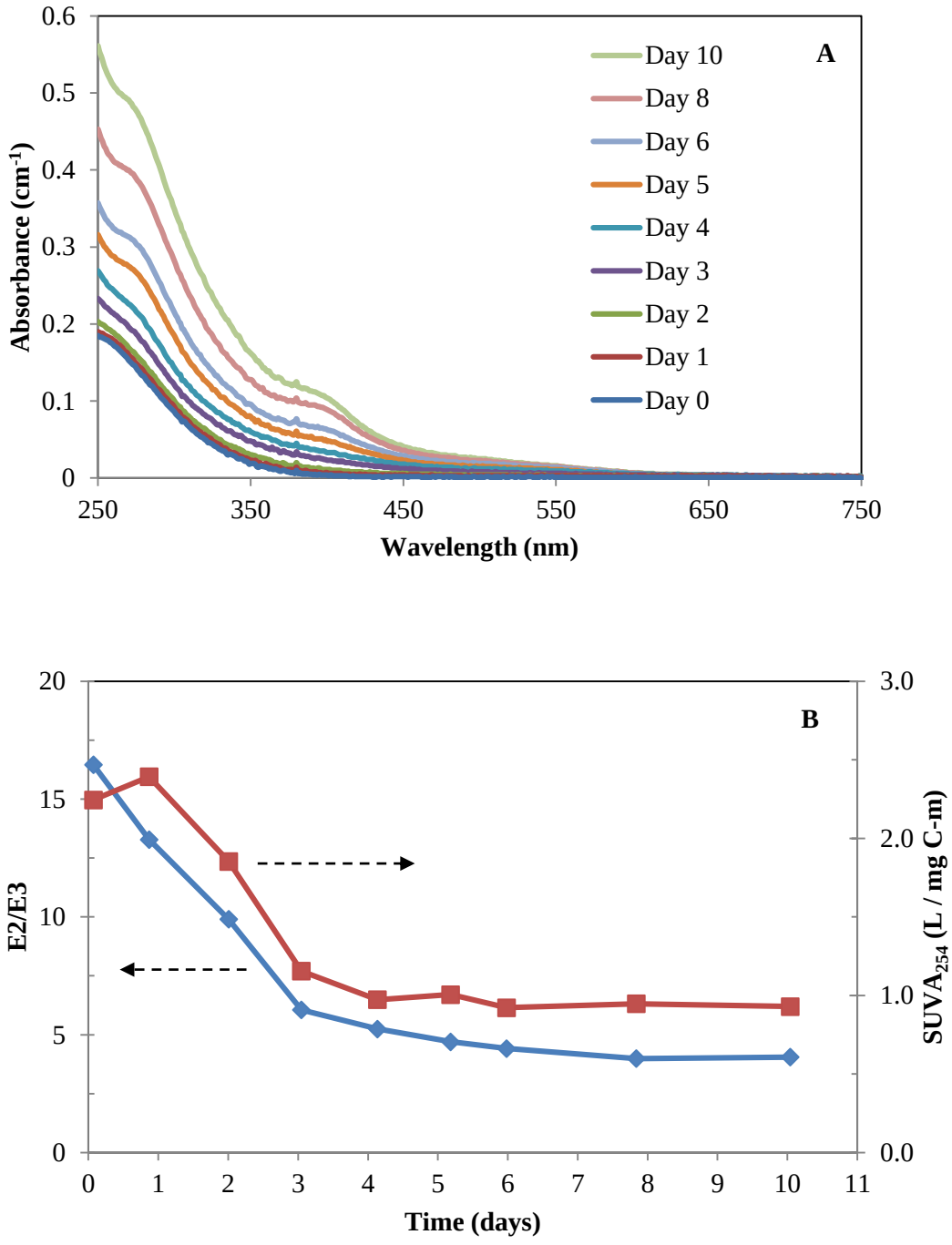

Figure 3: Optical and chemical properties of EOM solutions throughout *C. reinhardii* growth (A) UV-vis absorbance (B) E2/E3 ratios and SUVA at λ = 254 nm (C) Specific absorbance values for λ in the UV and visible spectrum.

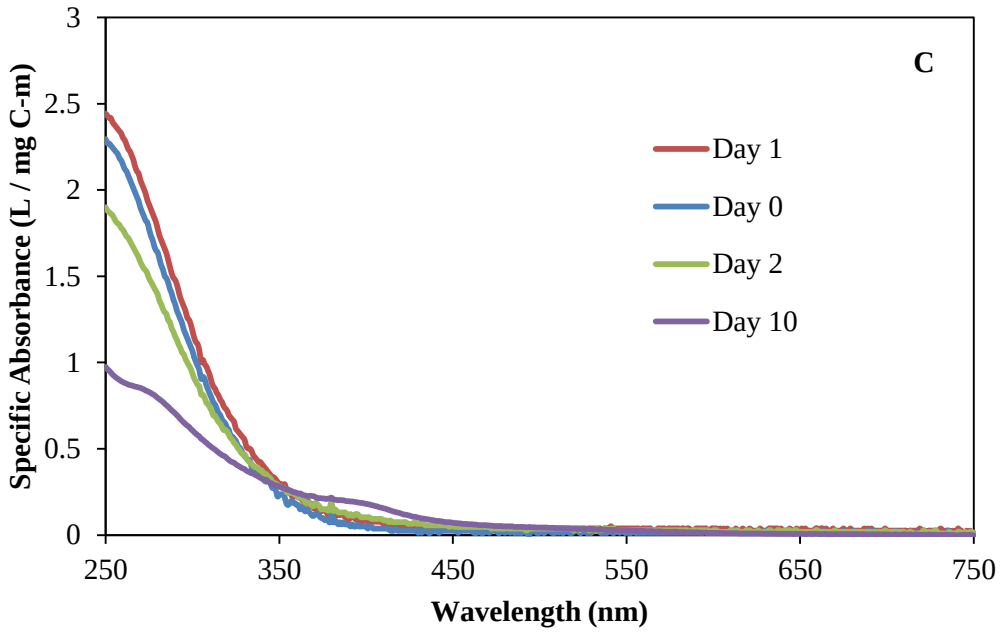

Figure 3 (cont.)

Figure 3A shows that EOM absorbance increases with increasing *C. reinhardtii* growth and increasing DOC allowing EOM to absorb light and participate in energy and electron transfer reactions inducing reactive species production (Richard and Canonica, 2005). Recent studies have investigated trends between optical properties such as E2/E3 ratios (absorbance at $\lambda = 254$ nm divided by absorbance at $\lambda = 365$ nm) to reactive species production (Dalrymple et al., 2010). For example E2/E3, was negatively related to $^1O_2$ quantum yields in natural DOM samples and terrestrial DOM isolates under the irradiation of a UVA mercury lamp (Dalrymple et al., 2010).

Figure 3B shows that E2/E3 ratios decrease throughout growth. E2/E3 ratios are known to correlate with aromaticity (Peuravuori and Pihlaja, 1997). Additionally, $SUVA_{254}$ (absorbance at $\lambda = 254$ nm divided by DOC in mg C/L) which also correlates with aromaticity, decreases throughout culture growth similar to the trend in E2/E3. It is surprising that increased production of reactive species throughout growth (described in Section 3.2 - 3.4) occurs with decreasing aromatic light-absorbing functional groups, but may be explained by the findings of AOM

characterization studies. For example, Henderson and coworkers saw that $SUVA_{254}$ only captured humic/fulvic aromaticity and did not encompass tryptophan and other amino acid aromaticity (Henderson et al., 2008). Interestingly, Figure 3C shows that although $SUVA_{254}$ may be decreasing throughout growth, absorbance normalized to DOC at wavelengths near $\lambda = 400$ nm ($SUVA_{400}$) increases with culture growth. Other EOM characterization techniques such as fluorescence excitation-emission matrices (EEMs) may provide additional insights into molecular properties of EOM that contribute to photoreactivity.

3.2 Solar •OH generation

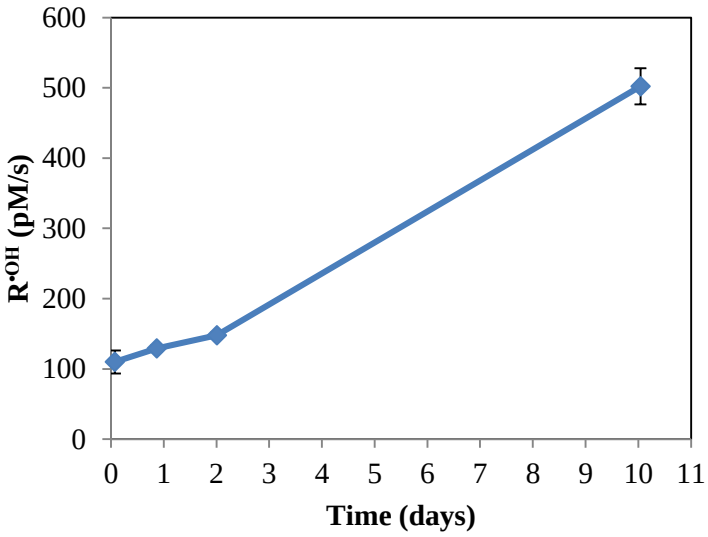

Figure 4: Reactive oxygen species quantification throughout *C. reinhardtii* growth. •OH formation rates ($R^{\bullet OH}$) (pM/s = 10^{-12} M/s). Values corrected for light screening.

Figure 4 shows $R^{\bullet OH}$ increasing with growth. It should be noted that $R^{\bullet OH}$ is a measure of •OH production in EOM and this measurement does not describe the •OH-quenching properties or •OH steady-state concentrations of EOM (Foote, 1995). Figure 4 shows that there is significant $R^{\bullet OH}$ at day 0. This is a result of •OH sensitizers in the growth media. Since the media contains both iron and EDTA ($[Fe^{3+}] = 20$ μM; [EDTA] = 58 μM), Fe^{3+}-EDTA complexes may form

which produce •OH under sunlight irradiation (Gutteridge et al., 1990). Therefore, the Fe^{3+}-EDTA complexes may explain the high $R^{\bullet OH}$ on day 0. The $R^{\bullet OH}$ increases by ~15% from day 0 to 1. The increase in $R^{\bullet OH}$ from day 1 to 2 is also ~15%. Overall, there is over a 4-fold increase in $R^{\bullet OH}$ after 10 days relative to the initial value. The data suggests that DOC from EOM is a sensitizer for •OH similarly to what has been shown for DOM in surface waters, DOM isolates, and wastewater (Dong and Rosario-Ortiz, 2012; Page et al., 2014).

A recent study showed that bulk wastewater samples from secondary effluent have a higher $R^{\bullet OH}$ than natural waters. $R^{\bullet OH}$ in wastewater samples (DOC = 6 – 7 mg C/L) ranged from 0.76×10^{-10} – 1.3×10^{-10} M/s with irradiance 71 W/m^2 from 290 – 400 nm (Dong and Rosario-Ortiz, 2012). The authors suggested that an extrapolation to irradiance = 44 W/m^2 from 290 – 400 nm (i.e., the irradiance of sunlight) is necessary to compare lab-scale $R^{\bullet OH}$ to sunlit natural water $R^{\bullet OH}$ (Dong and Rosario-Ortiz, 2012; Hulstrom et al., 1985). After extrapolation, $R^{\bullet OH}$ in wastewater is 4.71×10^{-11} – 8.05×10^{-11} M/s (Dong and Rosario-Ortiz, 2012). This is higher that the $R^{\bullet OH}$ in natural waters where DOC = 0.3 – 5.16 mg C/L and $R^{\bullet OH}$ is 10^{-12} – 10^{-11} M/s (Dong and Rosario-Ortiz, 2012; Nakatani et al., 2007; Vione et al., 2006). $R^{\bullet OH}$ values in EOM using simulated sunlight are between 1.1×10^{-10} – 5.02×10^{-10} M/s at an irradiance ~ 36 W/m^2 from 290 – 400 nm with DOC = 8.1 – 57.5 mg C/L. When we convert $R^{\bullet OH}$ to sunlight irradiance, the $R^{\bullet OH}$ range for EOM is 1.34×10^{-10} – 6.14×10^{-10} M/s. In this same study by Dong and Rosario-Ortiz, $R^{\bullet OH}$ contribution from nitrate in wastewater samples was subtracted from total production $R^{\bullet OH}$ production to elucidate $R^{\bullet OH}$ from wastewater effluent organic matter only (Dong and Rosario-Ortiz, 2012). If we modify the results we found in this study and subtract •OH production from day 0, believed to originate from Fe^{3+}-EDTA complex sensitizers and inoculum DOC, the $R^{\bullet OH}$ range becomes 0 – 3.92×10^{-10} M/s. After the calculation, $R^{\bullet OH}$ from *C. reinhardtii* EOM is higher than $R^{\bullet OH}$ in

both natural waters and effluent organic matter (Dong and Rosario-Ortiz, 2012). However, the DOC in EOM solutions is 8 times greater than wastewater and 11 times greater than natural water DOC. In current research, the •OH photogenerating and micropollutant degrading properties of wastewater effluent and wetlands are being evaluated (Dong and Rosario-Ortiz, 2012; Jasper and Sedlak, 2013; Ryan et al., 2011). Based on our results, we believe algal cultivation systems should also be evaluated for important processes such as micropollutant removal and pathogen inactivation due to •OH production that surpasses that of natural waters and wastewater secondary effluent. However, the conclusions we can obtain from these results are limited and a more complete investigation on EOM quenching properties is necessary which requires $[\bullet OH]_{ss}$ quantification. Understanding •OH production alone is not sufficient and further work investigation •OH steady-state levels is needed.

3.3 Solar ^{3}DOM generation

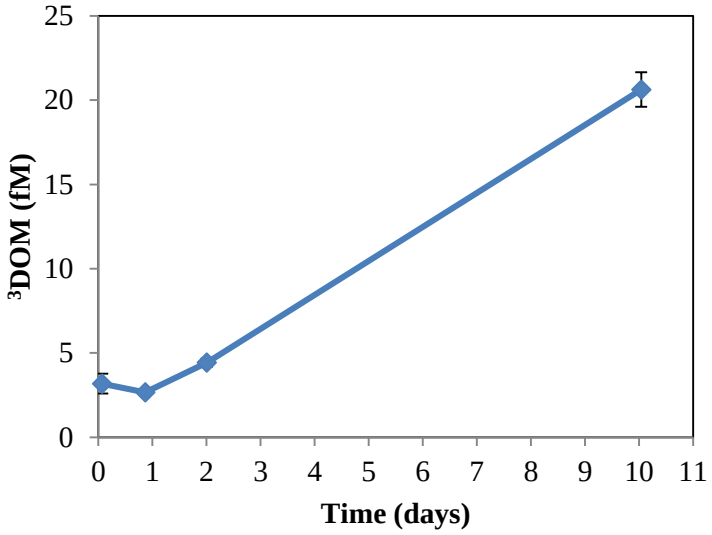

Figure 5: Reactive species quantification throughout *C. reinhardtii* growth. ^{3}DOM steady-state concentrations ($[^3DOM]_{ss}$) (fM = 10^{-15} M). Values Corrected for light screening.

Figure 5 shows that on day 0 where EDTA is the main organic carbon source (~6.9 mg C/L), there is still a measureable $[^3DOM]_{ss}$. $[^3DOM]_{ss}$ at day 0 originates from two potential sources. First, an overestimation of ^{3}DOM may originate from TMP decay as a result of oxidation by •OH generated from iron sensitizers (Gutteridge et al., 1990; Housari et al., 2010). Second, TMP may react with an excited triplet state of EOM from the inoculum i.e. the EOM originating from the backup culture. On Day 1, $[^3DOM]_{ss}$ is within the standard deviation of $[^3DOM]_{ss}$ measured on day 0, meaning there is no statistical difference between day 0 to 1 values. Between day 1 and 2, there is approximately a 65% increase in $[^3DOM]_{ss}$. Overall, there is a 5-fold increase in $[^3DOM]_{ss}$ after 10 days relative to the initial value.

TMP decays mainly in the presence of ^{3}DOM and has been used to quantify ^{3}DOM originating from terrestrial organic matter in natural waters, synthetic model photosensitizers, NOM isolates, and wastewater organic matter (Canonica and Hoigné, 1995; Canonica et al., 1995; Niu et al.,

2014; Parker et al., 2013; Rosado-Lausell et al., 2013). As *C. reinhardtii* grows, EOM becomes the dominant source of DOM. Approximately after day 4 of cultivation (Figure 2A), measured $[^3DOM]_{ss}$ values are assumed to be triplet excited states of extracellular organic matter (^3EOM). The existence of ^3EOM has been predicted by many authors but has not been measured until now (Ge et al., 2009; Liu et al., 2003; Peng et al., 2009; Wang et al., 2007). The $[^3DOM]_{ss}$ throughout growth ranged from $3.19 \times 10^{-15} – 2.06 \times 10^{-14}$ M for EOM solutions with DOC = 8.1 – 57.5 mg C/L. Grebel et al. found that $[^3DOM]_{ss}$ ranged from $4 \times 10^{-16} – 9 \times 10^{-16}$ M in SRNOM with DOC = 4 – 15 mg C/L (Grebel et al., 2011). Zepp and coworkers estimated $[^3DOM]_{ss}$ produced from humic substances with $A_{366} = 0.2$ in sunlit water bodies to be $10^{-15} – 10^{-13}$ M (Zepp et al., 1985a). For comparison, $A_{366} = 0.2$ corresponds to ~17 mg C/L for SRNOM. If we extrapolate solar simulator $[^3DOM]_{ss}$ produced from EOM to sunlight irradiance (44 W/m^2) (Hulstrom et al., 1985), the $[^3DOM]_{ss}$ range is $4.41 \times 10^{-15} – 2.85 \times 10^{-14}$ M. ^3DOM levels photogenerated from EOM fall within the range of those found by Zepp et al. and are higher than those measured by Grebel et al. (Grebel et al., 2011; Zepp et al., 1985a). Although $[^3DOM]_{ss}$ from EOM are comparable or slightly greater than reported values, the DOC needed to achieve such $[^3DOM]_{ss}$ is much greater. When comparing maximum values, DOC from EOM solutions is over 3-fold greater than DOC from SRNOM in Grebel et al. and estimated humic acid DOC in Zepp et al. (Grebel et al., 2011; Zepp et al., 1985b). Additionally, it should be noted that the steady-state values calculated in this and other studies are not quite comparable due to the use of different probes.

The sorbic acid probe used and developed by Grebel et al. reacts with ^3DOM via energy transfer reactions (Grebel et al., 2011; Parker et al., 2013). In another study, Zepp and coworkers used 1,3-pentadiene and 2,4-dimethyl furan as probes which react with ^3DOM also exclusively

through energy transfer reactions (Zepp et al., 1985a). TMP however, reacts with ^{3}DOM via electron transfer reactions (Dong and Rosario-Ortiz, 2012). Therefore, individual probes target different reactive properties of ^{3}DOM (Grebel et al., 2011). Nonetheless, the pool of ^{3}DOM detected by TMP is the same pool of ^{3}DOM involved with $^1O_2$ production (Halladja et al., 2007). A more direct comparison of our results can be made by a very recent study from Niu et al. where ^{3}DOM was measured using TMP in wastewater and fulvic acid isolates using a solar simulator (Niu et al., 2014). To make comparisons, $[^3DOM]_{ss}$ was estimated using the reported values for $k_{app,TMP}$ and $[^1O_2]_{ss}$ provided in Niu et al. In wastewater hydrophobic and transphilic fractions, the $[^3DOM]_{ss}$ averages were 8.7×10^{-15} M for 4 mg C/L and 1.1×10^{-14} M for 20 mg C/L. For fulvic isolates, the $[^3DOM]_{ss}$ averages were 1.2×10^{-14} M for 4 mg C/L and 1.0×10^{-14} M for 20 mg C/L. The $[^3DOM]_{ss}$ produced from EOM solutions in this study were slightly higher but similar to $[^3DOM]_{ss}$ measured in fulvic acid and wastewater isolates (Niu et al., 2014). However, the DOC needed to achieve these ^{3}DOM levels in EOM solutions was almost 3-fold greater than the wastewater and fulvic acid isolate solutions in Niu et al. when comparing maximum DOC concentrations. Regardless, the conclusion from this discovery about comparable $[^3DOM]_{ss}$ is that current knowledge about ^{3}DOM oxidation of sulfa drugs and other PPCPs in natural waters and NOM isolates can be directly applied to algal cultivation systems.

3.4 Solar $^1O_2$ generation

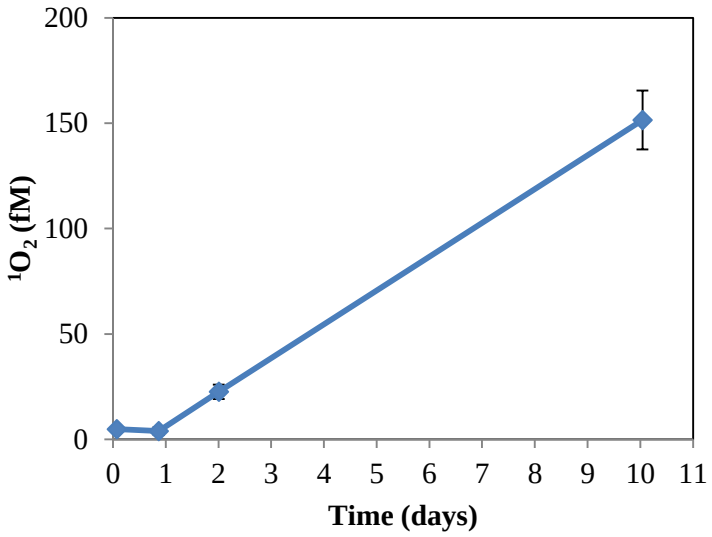

Figure 6: Reactive oxygen species quantification throughout *C. reinhardtii* growth. $^1O_2$ steady-state concentrations ($[^1O_2]_{ss}$) (fM = 10^{-15} M). Values corrected for light screening.

Figure 6 shows that there is measurable $[^1O_2]_{ss}$ on day 0 which can be explained by EOM sensitizers originating from the inoculum. From day 0 to day 1, $[^1O_2]_{ss}$ does not significantly change since it is still within the standard deviation of day 0. From day 1 to day 2, there is more than a 5-fold increase in $[^1O_2]_{ss}$. At day 10, there is over a 30-fold increase in $[^1O_2]_{ss}$ compared to day 0. Because $^1O_2$ originates from energy transfer reactions between ^{3}DOM and ground-state or dissolved oxygen ($^3O_2$) (Zepp et al., 1977), high $[^1O_2]_{ss}$ implies that sufficient ^{3}DOM were formed to produce these measured $^1O_2$ levels. This may explain the less dramatic increase in $[^3DOM]_{ss}$ over culture growth compared with $[^1O_2]_{ss}$ (Figure 5); ^{3}DOM is quenched by ground-state O_2 to produce the observed $^1O_2$ levels. $[^1O_2]_{ss}$ increases from 4.80×10^{-15} – 1.52×10^{-13} M throughout 10 days of growth at irradiance ~36 W/m^2 from 290 – 400 nm. In natural waters, $[^1O_2]_{ss}$ ranges from 10^{-13} – 10^{-12} M (Burns et al., 2012). Assuming the sunlight intensity is 44 W/m^2 in natural systems (Dong and Rosario-Ortiz, 2012; Hulstrom et al., 1985), an extrapolation of the EOM photogenerated $[^1O_2]_{ss}$ would be 5.88×10^{-15} – 1.56×10^{-13} M. Therefore, $[^1O_2]_{ss}$

generated in EOM fall within the range of $^1O_2$ expected in natural waters. An important conclusion from this result is that the knowledge of pathogen inactivation and micropollutant removal gained from previous studies in DOM from natural waters, wastewater, and NOM isolates can be applied to algal cultivation systems, supporting the need for further study in oxidation processes in biotechnology (Davies-Colley et al., 1999; Kohn and Nelson, 2007; Kohn et al., 2007; Mostafa and Rosario-Ortiz, 2013; Peterson et al., 2012; Romero et al., 2011; Scully Jr. and Hoigné, 1987).

3.5 Correlations between reactive species levels and EOM solution properties

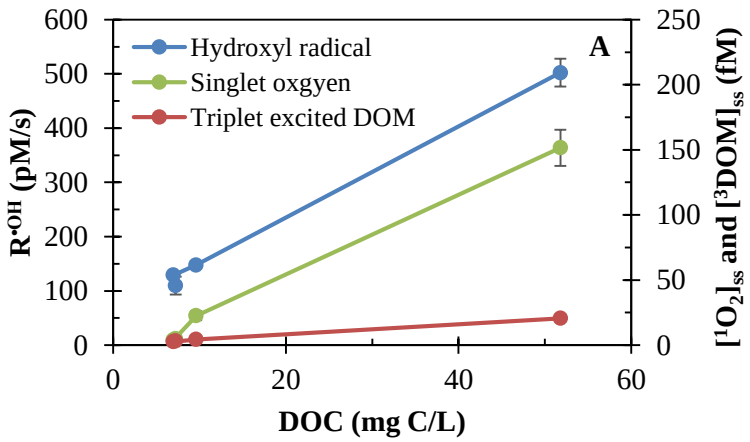

Figure 7: EOM sensitized reactive species levels and correlations with chemical and optical characteristics (A) DOC (B) $SUVA_{254}$ (C) $SUVA_{400}$ and (D) E2/E3.

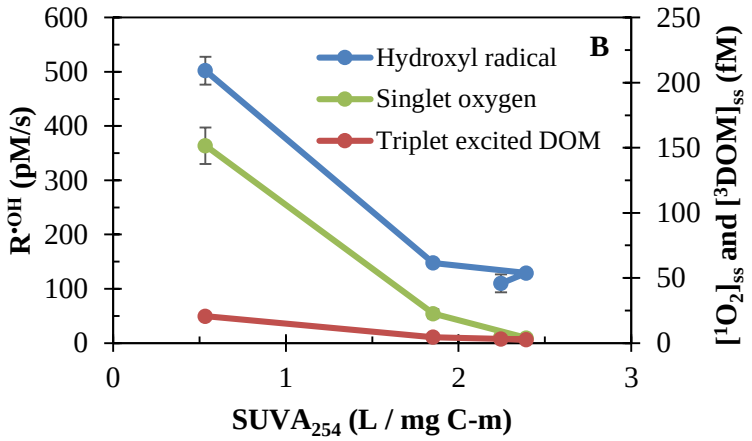

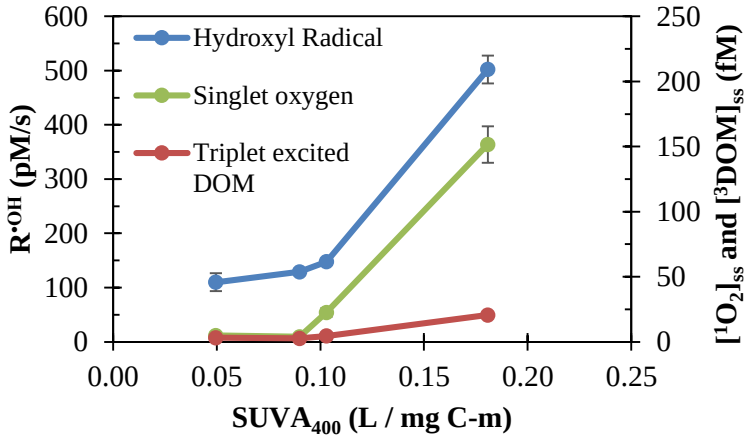

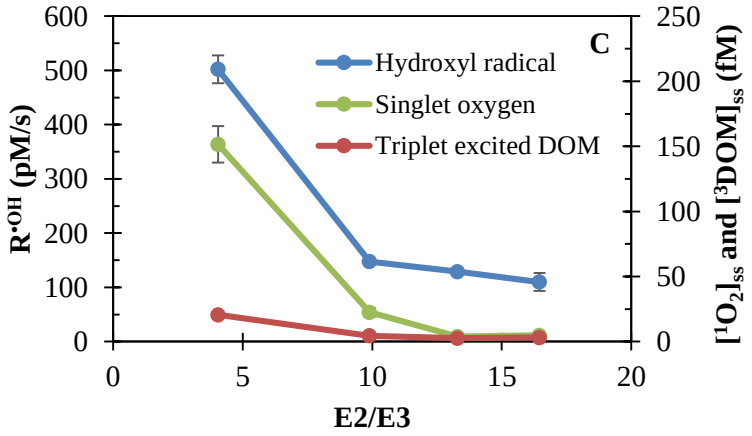

Figure 7 (cont.)

Figure 7A shows that all the reactive species stead-state concentrations and production rates increase with increasing DOC. Previous studies have shown that there is a linear correlation between organic matter DOC and $[^1O_2]_{ss}$. In a study by Kohn and coworkers, the slope of this trend was quantified for purified DOM isolates such as Fluka humic acid (FHA) (6.5×10^{-15} mol_{1O2}/mg NOM), Suwannee River humic acid (SRHA) (4×10^{-15} mol_{1O2}/mg DOM), , Aldrich humic acid (AHA) (1.3×10^{-14} mol_{1O2}/mg DOM), and Pony Lake fulvic acid (PFLA) (3.2×10^{-15} mol_{1O2}/mg DOM) (Kohn et al., 2007). The DOC-normalized $[^1O_2]$ for EOM in this study was 3.2×10^{-15} mol_{1O2}/mg DOM which most closely resembles the value from PLFA. PLFA is isolated from an Antarctic saline pond where the organic matter source originates primarily from dense blooms of *Chlamydomonas intermedia* Chodat. PLFA is known as an autochthonous or microbially derived organic matter (Brown et al., 2004). Considering the DOM solutions in this study originates mainly from the EOM of a microorganism also in the *Chlamydomonas* genus, it makes sense that normalized $^1O_2$ levels are so similar. Also, the data suggests terrestrially derived organic matter sources (FHA, SRHA, AHA) are better sensitizers for $^1O_2$ than microbially derived sources (Kohn and Nelson, 2007). Results from this study also support this comparison and will be discussed further in Section 3.5. In another previous study, it was shown that $[^3DOM]_{ss}$ quantified using the energy transfer probe (sorbic acid) and SRNOM DOC concentrations were positively correlated (Grebel et al., 2011). Similarly, the $[^3DOM]_{ss}$ quantified in this study using the energy transfer probe (TMP) and EOM were positively correlated. $R_{\bullet OH}$ in this study increase with increasing DOC and a similar trend was observed in a study where •OH formation rates were compared with DOC changes in several water bodies in the Arctic (Page et al., 2014).

Figure 7B shows that increasing levels of reactive species increase with decreasing $SUVA_{254}$, which is opposite of what has been shown in previous studies. One study found that $SUVA_{254}$ in several DOM isolates and natural water samples had a positive correlation with TMP first-order decay rates and $[^1O_2]_{ss}$ (Rosado-Lausell et al., 2013). Aromaticity is known to be positively correlated with reactive species production and also positively correlated with reactive species quenching (Rosado-Lausell et al., 2013; Wenk and Canonica, 2012). The unexpected inverse relationship between $SUVA_{254}$ and $[^1O_2]_{ss}$ and $[^3DOM]_{ss}$ in Figure 7B results from one of two possibilities. One is that the aromatic content which is responsible for reactive species sensitizing is not absorbed at $\lambda = 254$ nm, but at higher wavelengths such as aromatic amino acids like tryptophan (Henderson et al., 2008). Although $SUVA_{254}$ and humic/fulvic type aromaticity is decreasing, biological aromaticity may follow an alternate trend with increasing DOC. For example, Figure 7C shows that reactive species increases with increasing $SUVA_{400}$. In other words, the portion of DOC which absorbs light near $\lambda = 400$ nm becomes more prevalent with increasing growth where more reactive species are present and may be a better indicator for EOM photoreactivity. The second possibility for the inverse relationship between $SUVA_{254}$ and reactive species levels is that the aromaticity is decreasing with increasing growth, and so aromatic quenchers for ^3DOM at later stages of growth are at a minimum yielding higher $[^3DOM]_{ss}$ (Wenk and Canonica, 2012). Because $^1O_2$ forms from ^3DOM, lower $[^1O_2]_{ss}$ would also be expected (Boreen et al., 2005). However, aromatic quenching of •OH does not play a role in the $R^{\bullet OH}$ measurement. Excess benzene is added in for •OH reactions and is therefore the major scavenger for hydroxyl radicals outcompeting aromatic DOC (Vione et al., 2006).

Decreasing E2/E3 ratios correlate with increasing reactive species levels. This trend contradicts what has been observed in DOM isolates from natural waters where increasing E2/E3 ratios

produce greater $^1O_2$ quantum yields which are directly related with steady-state levels. E2/E3 values have an inverse relationship with terrestrial DOM molecular weight; therefore, lower molecular weight compounds are better sensitizers for $^1O_2$ (Dalrymple et al., 2010). In contrast, Figure 4C suggests that it is the higher molecular weight compounds in EOM that are better sensitizers for reactive species photogeneration. Previous research shows that there is a greater quantity and diversity of high molecular weight EOM for several species of green microalgae and cyanobacteria in stationary phase compared to exponential phase (Pivokonsky et al., 2014). So, it is reasonable to hypothesize that higher molecular weight EOM can be sensitizers for the reactive species generation. However, further study on this hypothesis is needed. A summary of the reactive species quantification data used for the discussion in Sections 3.2 – 3.5 is provided below in Figure 8 and Table 1 respectively.

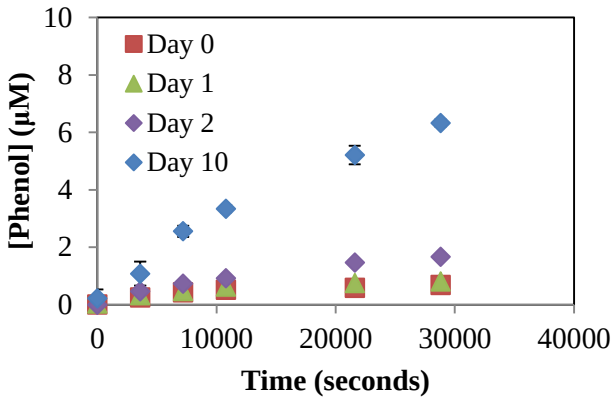

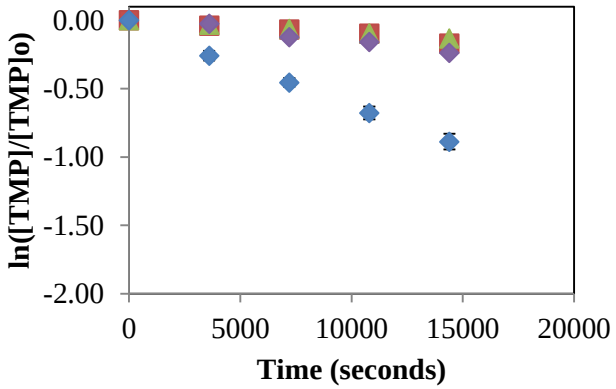

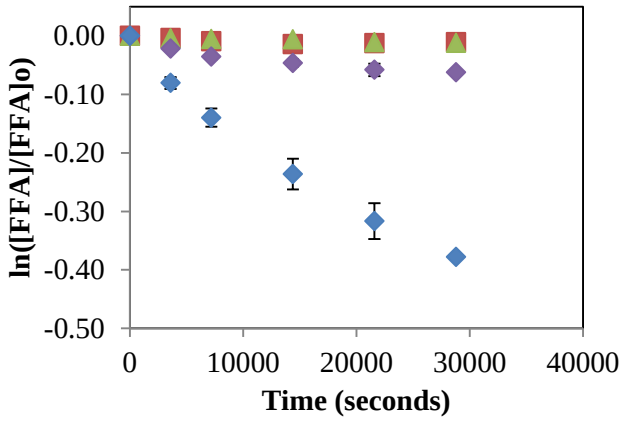

Figure 8: Raw data for •OH, ^{3}DOM, and $^1O_2$ quantification. Phenol production by benzene hydroxylation with •OH was measured; 2,4,6-trimethyl phenol and furfuryl alcohol decay due to reaction with ^{3}DOM and $^1O_2$, respectively, was measured.

Table 1: Summary of reactive oxygen species quantification throughout *C. reinhardtii* growth.

Species	[RS] Day 0	[RS] Day 1	[RS] Day 2	[RS] Day 10
$[^3DOM]$ (fM)	3.19 ± 0.58	2.67 ± 0.11	4.43 ± 0.23	20.63 ± 1.03
$[^1O_2]$ (fM)	4.80 ± 1.02	3.90 ± 1.80	22.55 ± 3.39	151.56 ± 13.96
$R^{\cdot OH}$ (pM/s)	109.89 ± 16.49	129.11 ± 4.75	147.75 ± 4.99	502.16 ± 25.71

Values were corrected for light screening. Standard deviations were calculated from triplicates. EOM water quality was diluted by 90% to accommodate probe stock solution volume. Solution conditions: $[DOC]_{Day\ 0}$ = 7.26 mg C/L; $[DOC]_{Day\ 1}$ = 7.00 mg C/L; $[DOC]_{Day\ 2}$ = 9.62 mg C/L; $[DOC]_{Day\ 10}$ = 51.78 mg C/L. Total Carbonate ($C_{T,CO3}$) varied for each sample. $[C_{T,CO3}]_{Day\ 0}$ = 8.14 mM; $[C_{T,CO3}]_{Day\ 1}$ = 8.88 mM; $[C_{T,CO3}]_{Day\ 2}$ = 5.38 mM; $[CT_{CO3}]_{Day\ 10}$ = 3.33 mM. pH fluctuated due to lack of buffer. $pH_{Initial}$ = 7.93 ± 0.08. pH_{Final} = 8.54 ± 0.33. RS = reactive species.

3.6 EOM vs. Terrestrial NOM

Table 2: A comparison of ^{3}DOM, $^1O_2$, and •OH generation in EOM at exponential phase with generation in the terrestrial organic matter surrogate Suwannee River Natural Organic Matter (SRNOM).

	EOM Matrix			EOM Matrix Corrected			SRNOM Matrix		
[^{3}DOM] (fM)	9.2	±	2.3	6.0	±	2.3	8.4	±	1.4
[$^1O_2$] (fM)	27.1	±	2.4	22.3	±	2.6	46.4	±	8.6
$R^{\bullet OH}$ (pM/s)	182.7	±	15.6	72.9	±	22.7	47.5	±	6.0

EOM Matrix sample harvested from time = 2.5 days representing late stationary phase. EOM water quality was diluted by 90% to accommodate space for probe stock solutions. EOM water quality was matched in SRNOM matrix using SRNOM isolate. DOC_{EOM} = $DOC_{EOM\ solution}$ (14 mg C/L) - DOC_{Media} (7 mg C/L)= 7 mg C/L. Solution conditions: DOC_{SRNOM} = 7 mg C/L; $C_{T,CO3}$ = 2.9 mM. $pH_{Initial}$ = 8.39 ± 0.12; pH_{Final} = 8.76 ± 0.18. IS_{EOM} ~ 12.6 mM; IS_{SRNOM} = 4 mM. $RS_{EOM,corrected}$ = $RS_{EOM,day\ 2.5}$ - $RS_{EOM,day\ 0}$

Table 2 shows the comparisons between EOM in exponential phase and SRNOM. EOM and SRNOM solutions were normalized to 7 mg C/L. However, EOM solutions contained an additional 7 mg C/L of EDTA included in the growth media. To more accurately compare EOM reactive species levels with SRNOM values, day 0 reactive species levels which contained media sensitizers were subtracted from the total EOM reactive species levels. $[^3DOM]_{ss}$ in EOM was similar to SRNOM levels, $[^1O_2]_{ss}$ in EOM was only 50% of the $^1O_2$ generated in SRNOM, and the $R^{\bullet OH}$ in EOM was comparable to SRNOM. This preliminary comparison suggests that when normalized to DOC, ^{3}DOM levels and •OH production are similar between EOM and SRNOM. The data in Table 2 also suggests SRNOM is a stronger sensitizer for $^1O_2$ than EOM and yields much higher $[^1O_2]_{ss}$. However, because this comparison only compares EOM from late exponential growth phase with SRNOM, a more in depth comparison between EOM at lag, exponential, and stationary growth phases and SRNOM at equivalent DOC concentrations is needed before this conclusion can be made.

It has been shown that EOM in exponential and stationary phase have distinct structural compositions including proteinaceous content and molecular weight distribution (Henderson et al., 2008; Pivokonsky et al., 2014). Whether these compositional differences correspond to different reactive species photogeneration has yet to be determined. To further investigate the relationship between growth phase and photogenerated reactive species in EOM, reactive species levels should be measured throughout culture growth more frequently during the 10 day growth period to gain insight about the optimal cultivation time that contains maximum reactive species levels. Additionally, comparisons to terrestrial organic matter must be made to determine whether substantial increases in reactive species levels throughout algal growth are attributed only to an increase in DOC or if there is a property inherent to EOM at specific growth phases that promotes enhanced reactive species photogeneration and deviates from expected linear trends. Using SRNOM sensitizers also provides a comparison to photochemistry occurring in sunlit natural waters. Since EOM water quality parameters have already been characterized throughout growth in this study, equivalent solutions containing similar water quality with SRNOM as the terrestrial DOC source can be made to compare photoreactivity.

CHAPTER 4: CONCLUSIONS

- There are significant increases in reactive species production (4-fold and up to 31-fold) in EOM solutions separated from a *C. reinhardtii* culture as biomass and DOC increased. Photoreactivity is enhanced throughout growth and further investigation is needed to optimize and improve the significant levels of reactive species in photobioreactors for tasks that may include pathogen and micropollutant removal.
- After detecting the growth phase with maximum reactive species production, further investigation into the EOM characteristics responsible for the enhanced performance is necessary. The positive correlation between $SUVA_{400}$ and reactive species levels shows that visible light absorbing organic matter may be important in reactive species production in EOM. Additionally, the inverse relationship between E2/E3 ratio and $SUVA_{254}$ with reactive species levels suggests humic/fulvic aromaticity does not participate in increased reactive species production as in aquatic and terrestrial DOM. More verification is needed to support the conclusion that higher molecular weight EOM are sensitizers for reactive species.
- A practical tool that can be obtained from this research is gaining the ability to easily measure bulk properties in EOM that can predict reactive species concentrations in cultivation systems, much like what has been done for $^1O_2$ in NOM isolates (Dalrymple et al., 2010). However, a deeper understanding of mathematical modeling and more frequent sampling throughout *C. reinhardtii* growth and subsequent reactive species quantification and EOM characterization is required.

REFERENCES

Andersen, R.A. (2005). Algal culturing techniques (Burlington, Mass: Elsevier/Academic Press).

Blough, N.V., and Zepp, R.G. (1996). Reactive Oxygen Species in Natural Waters. In Active Oxygen in Chemistry, C.S. Foote, J.S. Valentine, A. Greenberg, and J.F. Liebman, eds. (Springer Netherlands), pp. 280–333.

Boreen, A.L., Arnold, W.A., and McNeill, K. (2005). Triplet-Sensitized Photodegradation of Sulfa Drugs Containing Six-Membered Heterocyclic Groups: Identification of an SO2 Extrusion Photoproduct. Environ. Sci. Technol. *39*, 3630–3638.

Brown, A., McKnight, D.M., Chin, Y.-P., Roberts, E.C., and Uhle, M. (2004). Chemical characterization of dissolved organic material in Pony Lake, a saline coastal pond in Antarctica. Mar. Chem. *89*, 327–337.

Burns, J.M., Cooper, W.J., Ferry, J.L., King, D.W., DiMento, B.P., McNeill, K., Miller, C.J., Miller, W.L., Peake, B.M., Rusak, S.A., et al. (2012). Methods for reactive oxygen species (ROS) detection in aqueous environments. Aquat. Sci. *74*, 683–734.

Bushaw, K.L., Zepp, R.G., Tarr, M.A., Schulz-Jander, D., Bourbonniere, R.A., Hodson, R.E., Miller, W.L., Bronk, D.A., and Moran, M.A. (1996). Photochemical release of biologically available nitrogen from aquatic dissolved organic matter. Publ. Online 30 May 1996 Doi101038381404a0 *381*, 404–407.

Buxton, G.V., Greenstock, C.L., Helman, W.P., and Ross, A.B. (1988). Critical Review of rate constants for reactions of hydrated electrons, hydrogen atoms and hydroxyl radicals (·OH/·O− in Aqueous Solution. J. Phys. Chem. Ref. Data *17*, 513–886.

Canonica, S., and Freiburghaus, M. (2001). Electron-Rich Phenols for Probing the Photochemical Reactivity of Freshwaters. Environ. Sci. Technol. *35*, 690–695.

Canonica, S., and Hoigné, J. (1995). Enhanced oxidation of methoxy phenols at micromolar concentration photosensitized by dissolved natural organic material. Chemosphere *30*, 2365–2374.

Canonica, S., Jans, U., Stemmler, K., and Hoigne, J. (1995). Transformation Kinetics of Phenols in Water: Photosensitization by Dissolved Natural Organic Material and Aromatic Ketones. Environ. Sci. Technol. *29*, 1822–1831.

Chen, Y., Hu, C., Hu, X., and Qu, J. (2009). Indirect Photodegradation of Amine Drugs in Aqueous Solution under Simulated Sunlight. Environ. Sci. Technol. *43*, 2760–2765.

Cory, R.M., Cotner, J.B., and McNeill, K. (2009). Quantifying Interactions between Singlet Oxygen and Aquatic Fulvic Acids. Environ. Sci. Technol. *43*, 718–723.

Cory, R.M., McNeill, K., Cotner, J.P., Amado, A., Purcell, J.M., and Marshall, A.G. (2010). Singlet Oxygen in the Coupled Photochemical and Biochemical Oxidation of Dissolved Organic Matter. Environ. Sci. Technol. *44*, 3683–3689.

Dalrymple, R.M., Carfagno, A.K., and Sharpless, C.M. (2010). Correlations between Dissolved Organic Matter Optical Properties and Quantum Yields of Singlet Oxygen and Hydrogen Peroxide. Environ. Sci. Technol. *44*, 5824–5829.

Davies-Colley, R.., Donnison, A.., Speed, D.., Ross, C.., and Nagels, J.. (1999). Inactivation of faecal indicator micro-organisms in waste stabilisation ponds: interactions of environmental factors with sunlight. Water Res. *33*, 1220–1230.

Dong, M.M., and Rosario-Ortiz, F.L. (2012). Photochemical Formation of Hydroxyl Radical from Effluent Organic Matter. Environ. Sci. Technol. *46*, 3788–3794.

Dorfman, L.M., Taub, I.A., and Bühler, R.E. (2004). Pulse Radiolysis Studies. I. Transient Spectra and Reaction-Rate Constants in Irradiated Aqueous Solutions of Benzene. J. Chem. Phys. *36*, 3051–3061.

Eaton, A.D., Clesceri, L.S., Greenberg, A.E., Franson, M.A.H., American Public Health Association., American Water Works Association., and Water Environment Federation. (1995). Standard methods for the examination of water and wastewater (Washington, DC: American Public Health Association).

Elovitz, M.S., and von Gunten, U. (1999). Hydroxyl Radical/Ozone Ratios During Ozonation Processes. I. The Rct Concept. Ozone Sci. Eng. *21*, 239–260.

Foote, C.S. (1995). Active oxygen in chemistry (London; New York: Blackie Academic & Professional).

Ge, L., Deng, H., Wu, F., and Deng, N. (2009). Microalgae-promoted photodegradation of two endocrine disrupters in aqueous solutions. J. Chem. Technol. Biotechnol. *84*, 331–336.

Gerecke, A.C., Canonica, S., Müller, S.R., Schärer, M., and Schwarzenbach, R.P. (2001). Quantification of Dissolved Natural Organic Matter (DOM) Mediated Phototransformation of Phenylurea Herbicides in Lakes. Environ. Sci. Technol. *35*, 3915–3923.

De Godos, I., Muñoz, R., and Guieysse, B. (2012). Tetracycline removal during wastewater treatment in high-rate algal ponds. J. Hazard. Mater. *229-230*, 446–449.

Golanoski, K.S., Fang, S., Del Vecchio, R., and Blough, N.V. (2012). Investigating the Mechanism of Phenol Photooxidation by Humic Substances. Environ. Sci. Technol. *46*, 3912–3920.

Goldstone, J.V., and Voelker, B.M. (2000). Chemistry of Superoxide Radical in Seawater: CDOM Associated Sink of Superoxide in Coastal Waters. Environ. Sci. Technol. *34*, 1043–1048.

Goldstone, J.V., Pullin, M.J., Bertilsson, S., and Voelker, B.M. (2002). Reactions of Hydroxyl Radical with Humic Substances: Bleaching, Mineralization, and Production of Bioavailable Carbon Substrates. Environ. Sci. Technol. *36*, 364–372.

Grandbois, M., Latch, D.E., and McNeill, K. (2008). Microheterogeneous Concentrations of Singlet Oxygen in Natural Organic Matter Isolate Solutions. Environ. Sci. Technol. *42*, 9184–9190.

Grebel, J.E., Pignatello, J.J., and Mitch, W.A. (2011). Sorbic acid as a quantitative probe for the formation, scavenging and steady-state concentrations of the triplet-excited state of organic compounds. Water Res. *45*, 6535–6544.

Guerard, J.J., Miller, P.L., Trouts, T.D., and Chin, Y.-P. (2009). The role of fulvic acid composition in the photosensitized degradation of aquatic contaminants. Aquat. Sci. *71*, 160–169.

Guest, J.S., van Loosdrecht, M.C.M., Skerlos, S.J., and Love, N.G. (2013). Lumped Pathway Metabolic Model of Organic Carbon Accumulation and Mobilization by the Alga Chlamydomonas reinhardtii. Environ. Sci. Technol. *47*, 3258–3267.

Gutteridge, J.M., Maidt, L., and Poyer, L. (1990). Superoxide dismutase and Fenton chemistry. Reaction of ferric-EDTA complex and ferric-bipyridyl complex with hydrogen peroxide without the apparent formation of iron(II). Biochem. J. *269*, 169–174.

Haag, W.R., and Hoigne, J. (1986). Singlet oxygen in surface waters. 3. Photochemical formation and steady-state concentrations in various types of waters. Environ. Sci. Technol. *20*, 341–348.

Haag, W.R., Hoigne´, J., Gassman, E., and Braun, A. (1984). Singlet oxygen in surface waters — Part I: Furfuryl alcohol as a trapping agent. Chemosphere *13*, 631–640.

Halladja, S., ter Halle, A., Aguer, J.-P., Boulkamh, A., and Richard, C. (2007). Inhibition of Humic Substances Mediated Photooxygenation of Furfuryl Alcohol by 2,4,6-Trimethylphenol. Evidence for Reactivity of the Phenol with Humic Triplet Excited States. Environ. Sci. Technol. *41*, 6066–6073.

Henderson, R.K., Baker, A., Parsons, S.A., and Jefferson, B. (2008). Characterisation of algogenic organic matter extracted from cyanobacteria, green algae and diatoms. Water Res. *42*, 3435–3445.

Housari, F. al, Vione, D., Chiron, S., and Barbati, S. (2010). Reactive photoinduced species in estuarine waters. Characterization of hydroxyl radical, singlet oxygen and dissolved organic matter triplet state in natural oxidation processes. Photochem. Photobiol. Sci. *9*, 78–86.

Hulstrom, R., Bird, R., and Riordan, C. (1985). Spectral solar irradiance data sets for selected terrestrial conditions. Sol. Cells *15*, 365–391.

Janssen, E.M.L., Erickson, P.R., and McNeill, K. (2014). Dual roles of dissolved organic matter as sensitizer and quencher in the photooxidation of tryptophan. Environ. Sci. Technol.

Jasper, J.T., and Sedlak, D.L. (2013). Phototransformation of Wastewater-Derived Trace Organic Contaminants in Open-Water Unit Process Treatment Wetlands. Environ. Sci. Technol.

Kohn, T., and Nelson, K.L. (2007). Sunlight-Mediated Inactivation of MS2 Coliphage via Exogenous Singlet Oxygen Produced by Sensitizers in Natural Waters. Environ. Sci. Technol. *41*, 192–197.

Kohn, T., Grandbois, M., McNeill, K., and Nelson, K.L. (2007). Association with Natural Organic Matter Enhances the Sunlight-Mediated Inactivation of MS2 Coliphage by Singlet Oxygen. Environ. Sci. Technol. *41*, 4626–4632.

Leifer, A. (1988). The kinetics of environmental aquatic photochemistry: theory and practice (Washington, DC: American Chemical Society).

Li, L., Gao, N., Deng, Y., Yao, J., and Zhang, K. (2012). Characterization of intracellular & extracellular algae organic matters (AOM) of Microcystic aeruginosa and formation of AOM-associated disinfection byproducts and odor & taste compounds. Water Res. *46*, 1233–1240.

Liu, X., Wu, F., and Deng, N. (2004). Photoproduction of Hydroxyl Radicals in Aqueous Solution with Algae under High-Pressure Mercury Lamp. Environ. Sci. Technol. *38*, 296–299.

Liu, X.L., Wu, F., and Deng, N.S. (2003). Photodegradation of 17α-ethynylestradiol in aqueous solution exposed to a high-pressure mercury lamp (250 W). Environ. Pollut. *126*, 393–398.

Loiselle, S., Vione, D., Minero, C., Maurino, V., Tognazzi, A., Dattilo, A.M., Rossi, C., and Bracchini, L. (2012). Chemical and optical phototransformation of dissolved organic matter. Water Res. *46*, 3197–3207.

McGriff Jr., E.C., and McKinney, R.E. (1972). The removal of nutrients and organics by activated algae. Water Res. *6*, 1155–1164.

Minagawa, J. (2009). Chapter 14 - Light-Harvesting Proteins. In The Chlamydomonas Sourcebook (Second Edition), Elizabeth H. Harris, Ph.D., David B. Stern, Ph.D., and P.D. George B. Witman, eds. (London: Academic Press), pp. 503–539.

Mostafa, S., and Rosario-Ortiz, F.L. (2013). Singlet Oxygen Formation from Wastewater Organic Matter. Environ. Sci. Technol. *47*, 8179–8186.

Muñoz, R., and Guieysse, B. (2006). Algal–bacterial processes for the treatment of hazardous contaminants: A review. Water Res. *40*, 2799–2815.

Nakatani, N., Ueda, M., Shindo, H., Takeda, K., and Sakugawa, H. (2007). Contribution of the Photo-Fenton Reaction to Hydroxyl Radical Formation Rates in River and Rain Water Samples. Anal. Sci. *23*, 1137–1142.

Nguyen, M., Westerhoff, P., Baker, L., Hu, Q., Esparza-Soto, M., and Sommerfeld, M. (2005). Characteristics and Reactivity of Algae-Produced Dissolved Organic Carbon. J. Environ. Eng. *131*, 1574–1582.

Niu, X.-Z., Liu, C., Gutierrez, L., and Croué, J.-P. (2014). Photobleaching-induced changes in photosensitizing properties of dissolved organic matter. Water Res. *66*, 140–148.

Oswald, W.J. (1991). Introduction to advanced integrated wastewater ponding systems. Water Sci. Technol. *24*, 1–7.

Oswald, W.J. (1995). Ponds in the twenty-first century. Water Sci. Technol. *31*, 1–8.

Page, S.E., Logan, J.R., Cory, R.M., and McNeill, K. (2014). Evidence for dissolved organic matter as the primary source and sink of photochemically produced hydroxyl radical in arctic surface waters. Environ. Sci. Process. Impacts.

Parker, K.M., Pignatello, J.J., and Mitch, W.A. (2013). Influence of Ionic Strength on Triplet-State Natural Organic Matter Loss by Energy Transfer and Electron Transfer Pathways. Environ. Sci. Technol.

Peng, Z., Wu, F., and Deng, N. (2006). Photodegradation of bisphenol A in simulated lake water containing algae, humic acid and ferric ions. Environ. Pollut. *144*, 840–846.

Peng, Z., Yang, H., Wu, F., Wang, B., and Wang, Z. (2009). Microalgae-induced photodegradation of bisphenol F under simulated sunlight. In 3rd International Conference on Bioinformatics and Biomedical Engineering, iCBBE 2009, June 11, 2009 - June 13, 2009, (IEEE Computer Society), p. IEEE Engineering in Medicine and Biology Society; Gordon Life Science Institute; Fudan University; Beijing University of Posts and Telecommunications; Beijing Institute of Technology.

Petasne, R.G., and Zika, R.G. (1987). Fate of superoxide in coastal sea water. Publ. Online 05 Febr. 1987 Doi101038325516a0 *325*, 516–518.

Peterson, B.M., McNally, A.M., Cory, R.M., Thoemke, J.D., Cotner, J.B., and McNeill, K. (2012). Spatial and Temporal Distribution of Singlet Oxygen in Lake Superior. Environ. Sci. Technol. *46*, 7222–7229.

Peuravuori, J., and Pihlaja, K. (1997). Molecular size distribution and spectroscopic properties of aquatic humic substances. Anal. Chim. Acta *337*, 133–149.

Pivokonsky, M., Safarikova, J., Baresova, M., Pivokonska, L., and Kopecka, I. (2014). A comparison of the character of algal extracellular versus cellular organic matter produced by cyanobacterium, diatom and green alga. Water Res. *51*, 37–46.

Quaranta, M.L., Mendes, M.D., and MacKay, A.A. (2012). Similarities in effluent organic matter characteristics from Connecticut wastewater treatment plants. Water Res. *46*, 284–294.

Richard, C., and Canonica, S. (2005). Aquatic Phototransformation of Organic Contaminants Induced by Coloured Dissolved Natural Organic Matter. In Environmental Photochemistry Part II, P. Boule, D.W. Bahnemann, and P.K.J. Robertson, eds. (Springer Berlin Heidelberg), pp. 299–323.

Romero, O.C., Straub, A.P., Kohn, T., and Nguyen, T.H. (2011). Role of Temperature and Suwannee River Natural Organic Matter on Inactivation Kinetics of Rotavirus and Bacteriophage MS2 by Solar Irradiation. Environ. Sci. Technol. *45*, 10385–10393.

Rosado-Lausell, S.L., Wang, H., Gutiérrez, L., Romero-Maraccini, O.C., Niu, X.-Z., Gin, K.Y.H., Croué, J.-P., and Nguyen, T.H. (2013). Roles of singlet oxygen and triplet excited state of dissolved organic matter formed by different organic matters in bacteriophage MS2 inactivation. Water Res. *47*, 4869–4879.

Ryan, C.C., Tan, D.T., and Arnold, W.A. (2011). Direct and indirect photolysis of sulfamethoxazole and trimethoprim in wastewater treatment plant effluent. Water Res. *45*, 1280–1286.

Schwarzenbach, R.P., Gschwend, P.M., and Imboden, D.M. (2003). Environmental organic chemistry (Hoboken, N.J.: John Wiley & Sons).

Scully Jr., F.E., and Hoigné, J. (1987). Rate constants for reactions of singlet oxygen with phenols and other compounds in water. Chemosphere *16*, 681–694.

Sharpless, C.M. (2012). Lifetimes of Triplet Dissolved Natural Organic Matter (DOM) and the Effect of NaBH4 Reduction on Singlet Oxygen Quantum Yields: Implications for DOM Photophysics. Environ. Sci. Technol. *46*, 4466–4473.

Timko, S.A., Romera-Castillo, C., Jaffé, R., and Cooper, W.J. (2014). Photo-reactivity of natural dissolved organic matter from fresh to marine waters in the Florida Everglades, USA. Environ. Sci. Process. Impacts *16*, 866–878.

Tratnyek, P.G., and Hoigné, J. (1994). Photo-oxidation of 2,4,6-trimethylphenol in aqueous laboratory solutions and natural waters: kinetics of reaction with singlet oxygen. J. Photochem. Photobiol. Chem. *84*, 153–160.

U.S. Department of Energy (2010). National Algal Biofuels Technology Roadmap (U.S. Department of Energy).

Vione, D., Falletti, G., Maurino, V., Minero, C., Pelizzetti, E., Malandrino, M., Ajassa, R., Olariu, R.-I., and Arsene, C. (2006). Sources and Sinks of Hydroxyl Radicals upon Irradiation of Natural Water Samples. Environ. Sci. Technol. *40*, 3775–3781.

Voelker, B.M., Sedlak, D.L., and Zafiriou, O.C. (2000). Chemistry of Superoxide Radical in Seawater: Reactions with Organic Cu Complexes. Environ. Sci. Technol. *34*, 1036–1042.

Wang, L., Zhang, C., Wu, F., and Deng, N. (2007). Photodegradation of aniline in aqueous suspensions of microalgae. J. Photochem. Photobiol. B *87*, 49–57.

Wenk, J., and Canonica, S. (2012). Phenolic Antioxidants Inhibit the Triplet-Induced Transformation of Anilines and Sulfonamide Antibiotics in Aqueous Solution. Environ. Sci. Technol. *46*, 5455–5462.

Zafiriou, O.C., Joussot-Dubien, J., Zepp, R.G., and Zika, R.G. (1984). Photochemistry of natural waters. Environ. Sci. Technol. *18*, 358A – 371A.

Zepp, R.G., and Schlotzhauer, P.F. (1983). Influence of algae on photolysis rates of chemicals in water. Environ. Sci. Technol. *17*, 462–468.

Zepp, R.G., Wolfe, N.L., Baughman, G.L., and Hollis, R.C. (1977). Singlet oxygen in natural waters. Nature *267*, 421–423.

Zepp, R.G., Schlotzhauer, P.F., and Sink, R.M. (1985a). Photosensitized transformations involving electronic energy transfer in natural waters: role of humic substances. Environ. Sci. Technol. *19*, 74–81.

Zepp, R.G., Schlotzhauer, P.F., and Sink, R.M. (1985b). Photosensitized transformations involving electronic energy transfer in natural waters: role of humic substances. Environ. Sci. Technol. *19*, 74–81.

Zhang, J., Fu, D., and Wu, J. (2012). Photodegradation of Norfloxacin in aqueous solution containing algae. J. Environ. Sci. *24*, 743–749.

Zuo, Y., and Jones, R.D. (1997). Photochemistry of natural dissolved organic matter in lake and wetland waters—production of carbon monoxide. Water Res. *31*, 850–858.

APPENDIX A

A.1 Solar simulator characterization

Solar simulator irradiance was characterized by measuring light intensity using a spectroradiometer in 12 positions inside the solar simulator chamber. The spectroradiometer sensor was placed at each location and light intensity was obtained and the average of triplicate measurements was taken. The chamber area was divided into 12 evenly spaced positions to spatially characterize lamp irradiation. The 12 positions correspond with reactor spacing and are displayed in Table A.1.

Table A1: Top-down view of 12 reactor positions in the solar simulator chamber. The numbered squares represent evenly-spaced positions in the chamber where reactors are placed.

1	2	3	4
5	6	7	8
9	10	11	12

Front of Chamber

Table A.2 shows the average irradiance at each respective position in the solar simulator chamber. The average irradiance of the entire chamber was 361.1 ± 47.3 W/m^2 when the solar simulator was set to 400 W/m^2.

Table A2: Average irradiance of 12 reactor positions in solar simulator. Grid corresponds with numbered positions in Table A.1. Irradiance units are W/m^2 and were measured in triplicate.

309.42	308.37	286.77	281.78
382.85	390.35	390.49	372.97
394.65	413.45	410.55	391.05

Front of chamber

The six locations with the highest average irradiation were chosen to provide maximum light intensity for three TMP triplicate (locations 6, 9, 10) and three FFA triplicate (locations 7, 11, 12) experiments running simultaneously. The average irradiance of the six locations was 398.4 ± 9.7 W/m^2. Three borosilicate glass tubes used for benzene triplicate experiments were laid flat in the chamber evenly spaced with the bottom of tubes facing the front of the chamber. Assuming that the irradiance on the glass tubes is the average irradiance of locations 5 – 12, irradiance is 393.29 ± 12.50 W/m^2.

A.2 Reactive species quantification

In this study, we quantified steady-state concentrations of singlet oxygen ($^1O_2$), excited triplet dissolved organic matter (^{3}DOM), and hydroxyl radical production rates ($R^{\bullet OH}$). Here we describe quantification methods in detail for each reactive species (RS) using the methods described by Foote et al. (Foote, 1995). The following reaction scheme helps define variables in the subsequent kinetic equations.

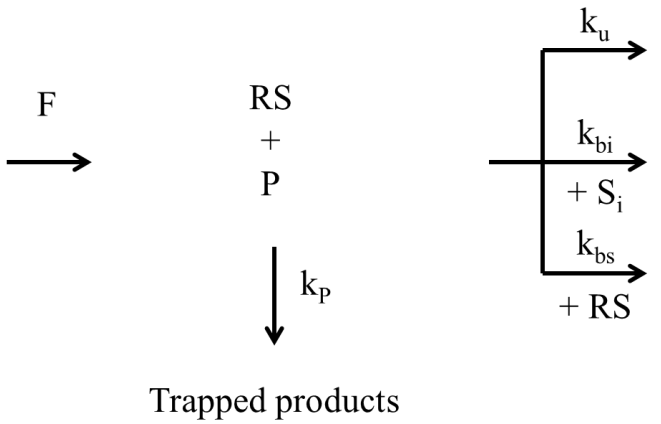

Figure A1: RS reaction scheme in water (Foote, 1995).

RS are first photogenerated at a constant rate F. Then, the RS can pass through various reaction pathways: (1) unimolecular decay with first-order rate constant k_u, (2) bimolecular reaction with other compounds S_i in water with second-order rate constant k_{bi}, (3) bimolecular self-reaction with second-order rate constant k_{bs}, and (4) bimolecular reaction with probe P with second-order rate constant k_p. RS self-reaction is negligible in natural waters and can be ignored. The relationship between all reactions can be described using the following equations.

$$\frac{d[RS]}{dt} = F - [RS]\left(k_u + k_p[P] + \sum_i k_{bi}[S_i]\right) \quad (6)$$

$$\frac{d[P]}{dt} = -k_p[RS][P] \quad (7)$$

After applying steady-state approximation ($\mathrm{d[RS]}/\mathrm{dt} = 0$) and rearranging equation 6, we obtain.

$$[RS]_{ss} = \frac{F}{k_u + k_p[P] + \sum_i k_{bi}[S_i]} \quad (8)$$

In this study, we quantified $^1O_2$ and ^{3}DOM using the first-order rate method and •OH using the initial formation rate method. The first-order method requires the use of probe concentrations

sufficiently low to leave $[RS]_{ss}$ unaffected ($k_p[P] \ll k_u + \sum_i k_{bi}[S_i]$). The rate of probe loss is then proportional to P.

$$\frac{d[P]}{dt} = -k_{app}[P] \tag{9}$$

$$k_{app} = k_p[RS]_{ss} \tag{10}$$

Integrating equation 9, we obtain

$$ln\frac{[P]}{[P]_0} = -k_{app}t \tag{11}$$

k_{app} is obtained from the slope after plotting $\ln[P]/[P]_0$ versus time. If k_p is known, then we can calculate $[RS]_{ss}$ using equation 10.

A.2.1 Singlet oxygen

Singlet oxygen requires the use of the first-order method. Furfuryl alcohol (FFA) reacts selectively with singlet oxygen and FFA decay can be measured over time. FFA decay is first-order with respect to $^1O_2$ and first order with respect to FFA making the reaction second order overall (Haag and Hoigne, 1986).

$$\frac{-d[FFA]}{dt} = k_{^1O_2,FFA}[^1O_2][FFA] \tag{12}$$

$$k_{^1O_2,FFA} = 1.2 \times 10^{-8} M^{-1}s^{-1} \tag{13}$$

Equation 12 follows pseudo first-order kinetics if [FFA] is sufficiently low to leave $[^1O_2]_{ss}$ constant. Under these conditions we obtain the following equation.

$$\frac{-d[FFA]}{dt} = k_{app}[FFA] \tag{14}$$

$$k_{app} = k_{^1O_2,FFA}[^1O_2]_{ss} \tag{15}$$

In equation 14, k_{app} is the apparent first-order rate constant. Integrating equation 14, we obtain

$$ln\frac{[FFA]}{[FFA]_o} = -k_{app}t \tag{16}$$

k_{app} is obtained from the slope after plotting $ln\frac{[FFA]}{[FFA]_o}$ versus time. Dividing k_{app} by $k_{^1O_2,FFA}$ gives the steady-state singlet oxygen concentration.

$$[^1O_2]_{ss} = \frac{k_{app}}{k_{^1O_2,FFA}} \tag{17}$$

A.2.2 Excited triplet dissolved organic matter

Steady-state excited triplet dissolved organic matter (^{3}DOM) quantification requires the use of the first-order method. 2,4,6-trimethyl phenol (TMP) decays in the presence of ^{3}DOM and can also decay in the presence of $^1O_2$. Side reactions with $^1O_2$ were avoided by using TMP in its protonated form (pK_a = 10.44; pH ~ 8), however we take into account potential $^1O_2$ oxidation as a conservative measure. •OH can also oxidize TMP but this reaction was negligible in studies investigating irradiated humic acid and fulvic acid solutions (Canonica and Freiburghaus, 2001). Therefore, we assume that TMP is oxidized by ^{3}DOM and $^1O_2$ only.

$$\frac{-d[TMP]}{dt} = k_{^3DOM,TMP}[^3DOM][TMP] + k_{^1O_2,TMP}[^1O_2][TMP] \tag{18}$$

After applying pseudo first-order kinetics to equation 18, we obtain the following.

$$\frac{-d[TMP]}{dt} = k_{app}[TMP] \tag{19}$$

$$k_{app} = k_{^3DOM,TMP}[^3DOM]_{ss} + k_{^1O_2,TMP}[^1O_2]_{ss} \tag{20}$$

Where $k_{^3DOM,TMP}$ is the second-order rate constant between ^{3}DOM and TMP ($k_{^3DOM,TMP}$ = 3.4 × 10^9 $M^{-1}s^{-1}$) and $k_{^1O_2,TMP}$ is the second-order rate constant between $^1O_2$ and TMP ($k_{^1O_2,TMP}$ = 6.2 × 10^7 $M^{-1}s^{-1}$) (Canonica et al., 1995; Tratnyek and Hoigné, 1994). We make the assumption that the ^{3}DOM that react with TMP have a second-order rate constant that is the average of benzophenone and 3'-methoxy acetophenone, two model ^{3}DOM sensitizers. Integrating equation 19 we obtain the following.

$$ln\frac{[TMP]}{[TMP]_o} = -k_{app}t \tag{21}$$

k_{app} is obtained from the slope after plotting $\ln\frac{[TMP]}{[TMP]_o}$ versus time. k_{app}, $k_{^3DOM,TMP}$, $k_{^1O_2,TMP}$, and $[^1O_2]_{ss}$ are all known, so $[^3DOM]_{ss}$ can be calculated as follows.

$$[^3DOM]_{ss} = \frac{k_{app} - k_{^1O_2,TMP}[^1O_2]_{ss}}{k_{^3DOM,TMP}} \tag{22}$$

A.2.3 Hydroxyl radical

4-chlorobenzoic acid is a molecular probe commonly used for $[•OH]_{ss}$ quantification (Elovitz and von Gunten, 1999; Jasper and Sedlak, 2013). Negligible pCBA decay occurred in irradiated extracellular organic matter (EOM) solutions preventing $[•OH]_{ss}$ quantification. Instead, the presence of •OH was investigated by quantifying hydroxyl radical production rates ($R^{•OH}$) using benzene as a molecular probe. Benzene reacts with •OH to yield a stable phenol product that can be measured over time (Vione et al., 2006). Benzene produced measurable concentrations of

phenol throughout irradiation for all samples in this study allowing for comparison. Below is the procedure used to quantify $R^{\bullet OH}$.

From phenol measurements, we can obtain a phenol production rate ($\frac{\mathrm{d[phenol]}}{\mathrm{dt}}$). The second-order rate constant between benzene and •OH is known ($k_{\bullet OH,benzene} = 7.8 \times 10^9 M^{-1}s^{-1}$) and benzene to phenol conversion efficiency is 0.85 (Dong and Rosario-Ortiz, 2012).

$$\frac{d[phenol]}{dt} = 0.85 \cdot k_{\bullet OH,benzene}[\bullet OH][benzene] \tag{23}$$

Applying the steady-state approximation to •OH formation rates leads to the following equation.

$$\frac{d[\bullet OH]}{dt} = 0 = R^{\bullet OH} - k_{\bullet OH,benzene}[\bullet OH][benzene] - \sum_i k_{\bullet OH,S_i}[\bullet OH][S_i] \tag{24}$$

S_i scavenges •OH with second-order rate constant $k_{\bullet OH,S_i}$. After rearranging equation 24 we obtain the following equation.

$$[\bullet OH]_{ss} = \frac{R^{\bullet OH}}{k_B[benzene] + \sum_i k_{S_i}[S_i]} \tag{25}$$

Substituting equation 25 into equation 23, we obtain the following.

$$\frac{d[phenol]}{dt} = 0.85 \cdot k_B[\bullet OH][benzene] = \frac{0.85 \cdot k_B \cdot R^{\bullet OH} \cdot [benzene]}{k_B[benzene] + \sum_i k_{S_i}[S_i]} \tag{26}$$

Utilizing a benzene concentration sufficiently high such that $k_B[benzene] \gg \sum_i k_{S_i}[S_i]$, equation 26 simplifies to.

$$R^{\bullet OH} = 0.85 \cdot \frac{d[phenol]}{dt} \tag{27}$$

So it is possible to obtain $R^{\bullet OH}$ from the initial formation rate of phenol.

A.3 Light-Screening Correction Factor

Steady-state singlet oxygen ($[^1O_2]_{ss}$) and excited triplet dissolved organic matter ($[^3DOM]_{ss}$) concentrations and hydroxyl radical formation rates ($R^{\bullet OH}$) were corrected for light-screening effects. Here we provide the derivation for light screening correction factors as described by Grandbois et al. (Grandbois et al., 2008).

Increasing dissolved organic matter (DOM) concentrations reduces quantified RS levels due to organic matter light screening, so RS must be corrected. The screening factor is a comparison of light intensity the surface of a solution with the average light intensity over a given solution thickness. The rate of light absorption for a thin solution ($k_{obs,thin}$) is defined as

$$k_{obs,thin} = 2.303 \sum_{\lambda} \alpha_\lambda I_\lambda \quad (1)$$

where λ is the wavelength, α_λ is the absorption coefficient at given wavelength (cm^{-1}), and I_λ is the surface irradiance at a given wavelength (W/m^2 nm). The rate of light absorption for a solution ($k_{obs,thick}$) with thickness z (cm) is defined as

$$k_{obs,thick} = 2.303 \sum_{\lambda} \alpha_\lambda \langle I_\lambda \rangle_z \quad (2)$$

where $\langle I_\lambda \rangle_z$ is the average irradiance over a thick solution with thickness z. $\langle I_\lambda \rangle_z$ is calculated by multiplying the surface irradiance I_λ by the light screening factor S_λ.

$$S_\lambda = \frac{1 - 10^{-\alpha_\lambda z}}{2.303 \alpha_\lambda z} \quad (3)$$

$$\langle I_\lambda \rangle_z = I_\lambda S_\lambda = I_\lambda \frac{1 - 10^{-\alpha_\lambda z}}{2.303 \alpha_\lambda z} \quad (4)$$

α_λ was obtained using a spectrophotometer (Schwarzenbach et al., 2003). z was obtained by measuring the solution thickness in glass tubes for benzene experiments and beakers for TMP and FFA experiments. To obtain light screening correction factors (CF), we divide $k_{obs,thin}$ by $k_{obs,thick}$.

$$CF = \frac{k_{obs,thin}}{k_{obs,thick}} = \frac{\sum_\lambda \alpha_\lambda I_\lambda}{\sum_\lambda \alpha_\lambda I_\lambda S_\lambda} \quad (5)$$

Corrected $[RS]_{ss}$ are obtained simply by multiplying measured $[RS]_{ss}$ by CF. Below is an example calculation for obtaining light-screening CFs as shown in Romero et al. where the derivation by Grandbois et al. was also used (Grandbois et al., 2008; Romero et al., 2011).

Table A3: Light-screening correction factor sample calculations.

z_{Tube} (cm)	1.041
z_{Beaker} (cm)	2.699

$k_{obs,thin}$	$k_{obs,thick}$	
0.87	0.85	0.83

Wavelength (nm)	Irradiance (I_λ) (W/m^2 nm)	Abs. (α_λ) Day 0 EOM	S_λ Tube	S_λ Beaker	$\alpha_\lambda * I_\lambda$	$\alpha_\lambda * I_\lambda * S_\lambda$ Tube	$\alpha_\lambda * I_\lambda * S_\lambda$ Beaker
251	2.51	0.183	8.09E-01	5.97E-01	4.03E-04	3.26E-04	2.41E-04
252	2.52	0.183	8.09E-01	5.97E-01	4.30E-04	3.48E-04	2.57E-04
253	2.53	0.182	8.10E-01	5.99E-01	4.67E-04	3.79E-04	2.80E-04
254	2.54	0.181	8.11E-01	6.00E-01	4.08E-04	3.31E-04	2.45E-04
255	2.55	0.180	8.12E-01	6.02E-01	5.04E-04	4.09E-04	3.03E-04
256	2.56	0.179	8.13E-01	6.03E-01	4.86E-04	3.95E-04	2.93E-04
257	2.57	0.178	8.14E-01	6.05E-01	4.83E-04	3.93E-04	2.92E-04
258	2.58	0.176	8.16E-01	6.08E-01	5.20E-04	4.24E-04	3.16E-04
259	2.59	0.175	8.17E-01	6.09E-01	5.72E-04	4.67E-04	3.49E-04
260	2.60	0.173	8.18E-01	6.13E-01	5.13E-04	4.20E-04	3.14E-04

Irradiance was obtained using spectroradiometer and applying a 280 nm longpass filter. Absorbance was obtained using spectrophotometer. Actual spreadsheet contains calculations from wavelengths 250 – 750 nm.

A.4 Experimental data

Table A4: RS quantification raw data for EOM vs. time and SRNOM comparison.

		FFA k_{app} (h^{-1})	$[^1O_2]_{ss}$ (fM)	TMP k_{app} (h^{-1})	$[^3DOM]_{ss}$ (fM)	d[phenol]/dt (pM/s)	$R^{\bullet OH}$ (pM/s)	DOC (mg C/L)
EOM vs. time	Day 0	0.0025	5.8	0.0382	3.0	82.5	97.1	7.26
		0.0015	3.5	0.0298	2.4	81.2	95.5	
		0.0019	4.5	0.0465	3.7	111.0	130.6	
	Day 1	0.0026	5.9	0.0309	2.5	106.8	125.7	7.00
		0.0016	3.6	0.0318	2.5	103.2	121.4	
		0.0007	1.7	0.0340	2.7	112.8	132.7	
	Day 2	0.0090	20.8	0.0598	4.5	119.1	140.2	9.62
		0.0111	25.7	0.0563	4.2	121.4	142.8	
		0.0077	17.9	0.0532	4.0	128.9	151.6	
	Day 10	0.0566	130.9	0.2384	17.3	407.9	479.9	51.78
		0.0527	122.1	0.2145	15.4	360.0	423.5	
		0.0451	104.5	0.2226	16.0	389.6	458.3	
EOM vs. SRNOM	EOM	0.0120	27.8	0.1148	8.9	170.1	200.2	7 (EOM) 12.9 (Total)
		0.0118	27.4	0.1454	11.4	139.7	164.4	
		0.0099	22.8	0.0803	6.1	147.0	172.9	
	SRNOM	0.0187	43.3	0.1138	8.6	35.9	42.2	7
		0.0203	46.9	0.1015	7.6	33.6	39.6	
		0.0129	29.8	0.0785	5.7	44.8	52.7	

A.5 Photobioreactor schematic

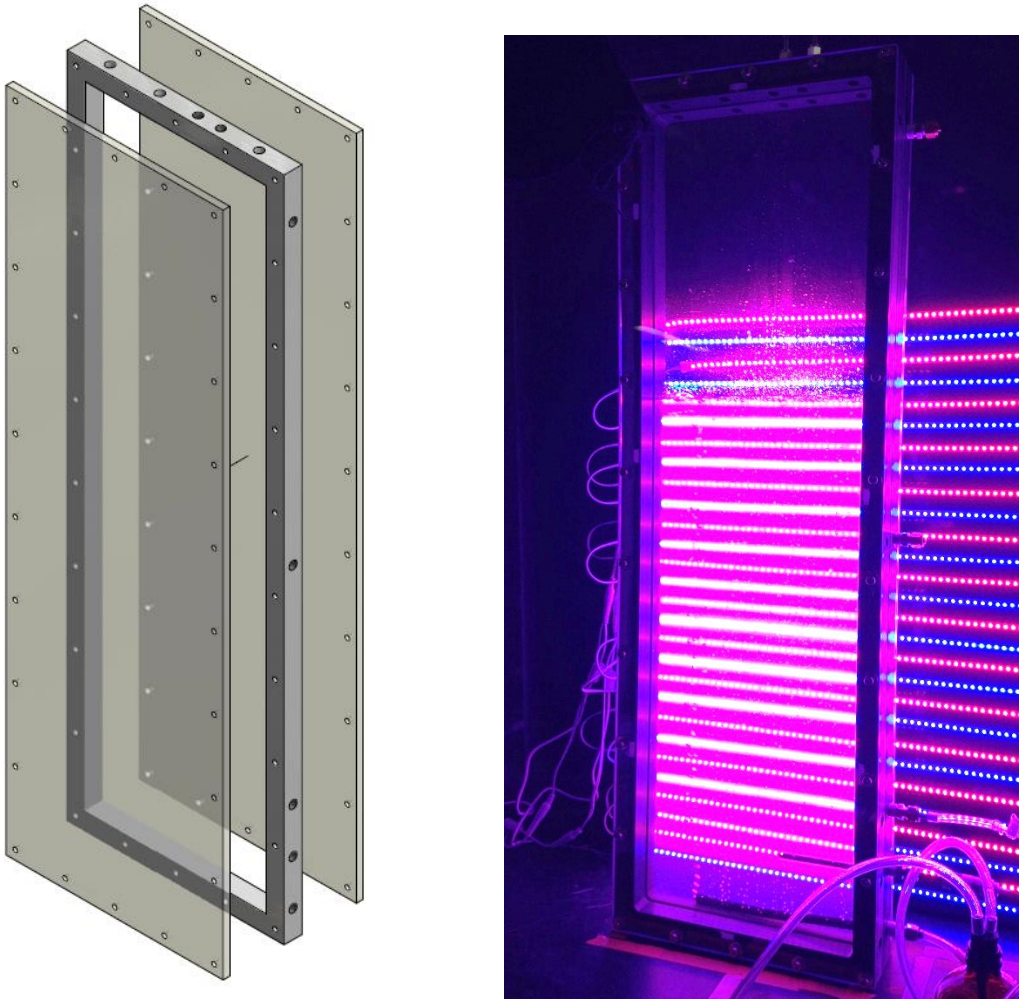

Figure A2: Photobioreactor schematic (left) and photo (right). Figure provided by Jennifer Debellis.